SRI International

Final Report • August 1996

PRODUCTS OF DISSOCIATIVE RECOMBINATION IN THE IONOSPHERE

Philip Cosby
Molecular Physics Laboratory

SRI Project 4810
MP 96-113

Prepared for:

National Aeronautics and Space Administration
Washington, DC 20546-0001
Dr. Mary Mellott, Code SS

Approved:

David Crosley
Director
Molecular Physics Laboratory

David M. Golden
Senior Vice President
Science and Technology Group

333 Ravenswood Avenue • Menlo Park, CA 94025-3493 • (415) 326-6200 • FAX: (415) 326-5512 • Telex: 334486

CONTENTS

INTRODUCTION

SRI International undertook a novel experimental measurement of the product states formed by dissociative recombination (DR) of O_2^+, NO^+, and N_2^+ as a function of both electron energy and reactant ion vibrational level. For these measurements we used a recently developed experimental technique for measuring dissociation product distributions that allows both the branching ratios to be accurately determined and the electronic and rovibrational state composition of the reactant ions to be specified.

DR is the dominant electron loss mechanism in all regions of the ionosphere. In this process, electron attachment to the molecular ion produces an unstable neutral molecule that rapidly dissociates. For a molecular ion such as O_2^+, the dissociation recombination reaction is

$$O_2^+ + e \rightarrow O + O + W \ . \qquad (1)$$

The atomic products of this reaction, in this case two oxygen atoms, can be produced in a variety of excited states and with a variety of kinetic energies, as represented by W in Eq. (1). These atoms are not only active in the neutral chemistry of the ionosphere but are also especially important because their optical emissions are often used to infer *in situ* concentrations of the parent molecular ion and ambient electron densities. Many laboratory measurements have been made of DR reaction rates under a wide range of electron temperatures, but very little is known about the actual distributions among the final states of the atomic products. This lack of knowledge seriously limits the validity and effectiveness of efforts to model both natural and man-made ionospheric disturbances. Bates[1] recently identified major deficiencies in the currently accepted branching ratios for O_2^+ as they relate to blue and green line emission measurements in the nocturnal F-region.

During our two-year effort, we partially satisfied our ambitious goals. We constructed and operated a variable pressure, electron-impact ion source and a high pressure, hollow-cathode discharge ion source for O_2^+, NO^+, and N_2^+ beams. Translational spectroscopy of the products of dissociative charge transfer in Cs vapor was used to accurately assay the composition of the O_2^+ and NO^+ beams and to develop a methodology for the vibrationally controlled preparation of the ground state ion beams. Attempts to assay the N_2^+ beam revealed a novel two-electron process in the charge transfer reactions.[2-4] A coaxial electron gun for the DR measurements was constructed following an extensive numerical design of the fields.

Tests of the gun, however, found substantial perturbations of the magnetic fields by the soft iron (CMI-C) assembly containing the Langmuir probe that locates the electron beam. Hydrogen annealing of the iron failed to eliminate the field perturbations, necessitating the removal of the probe assembly. During this work on the coaxial electron gun, we discovered that predissociated high Rydberg states of O_2 could be produced by subjecting the molecules to a sudden perturbation by an electromagnetic field. This technique allowed a measurement of the product branching to the atomic limits for the lowest seven vibrational levels of O_2^+.

ACCOMPLISHMENTS

We wrote two articles as a result of support from the Space Physics program. The first of these is being published, the second is being submitted for publication. A third article is in final preparation. We provide summaries of these articles below. Preprints of the first two articles are included as appendices.

(1) H. Helm, I. Hazell, C. W. Walter, and P. C. Cosby, On the Dissociative Recombination of O_2^+, in *Dissociative Recombination: Theory, Experiment, and Applications III*, edited by D. Zajfman, J. B. A. Mitchell, D. Schwalm, and B. R. Rowe (World Scientific, Singapore, 1996).

A critical review by Bates[1] of $O(^1D)$ and $O(^1S)$ production in the nocturnal F-region found glaring inconsistencies among the values of the $O(^1S)$ branching ratios from O_2^+ DR deduced from the Visible Airglow Experiment,[5] the equatorial F-region profile,[6] the Artificial Auroral Experiment Precede,[7] laboratory measurements,[8,9] and *ab initio* calculations.[10,11] We were able to address this problem by experimentally measuring the branching to $O(^1S)$, $O(^1D)$, and $O(^3P)$ atomic products produced by dissociation of the high O_2 Rydberg states formed in the DR, with full resolution of individual vibrational contributions.

Theory[11] predicts a yield of $O(^1S)$ (relative to a yield of 2 for all atoms) of 0.0024 for $v^+ = 0$, 0.051 for $v^+ = 1$, and 0.15 for $v^+ = 2$. This vibrational sensitivity is primarily a consequence of the location of the continuum state that is expected to contribute most strongly to the DR reaction. Generally higher yields are deduced from satellite-based observations,[12] which also predict an increase in the yield with vibrational quantum number. By comparison, our experimental yields for $O(^1S)$ increase only slightly for v = 0-2, with values of 0.033, 0.041, and 0.045, respectively, and actually decrease for the higher vibrational levels, in marked contrast to the vibrational dependence that is currently accepted. On the other hand, our experimental yields for $O(^1D)$ range from 0.73 to 0.82 in the lowest seven vibrational levels. Previous laboratory and

satellite-based observations place this yield near unity,[12] consistent with our more precise branching values. Queffelec et al.[9] determined quantum yields in the DR of vibrationally hot oxygen molecular ions. Their results of 0.44 for $O(^1S)$ and 0.96 for $O(^1D)$ are higher than the results of our study.

(2) P. C. Cosby, A. B. van der Kamp, and W. J. van der Zande, Dissociative Charge Transfer of NO^+, J. Chem. Phys. (submitted for publication).

The NO^+ molecular ion is notorious for its many, long-lived, electronically excited states that complicate measurements of this species in ion beams. We applied translational spectroscopy to the predissociated Rydberg states of NO that are produced by charge-transfer neutralization of NO^+ in Cs vapor. Production of these Rydberg states on the ground and excited state ion cores reflects the relative populations of the corresponding states in the NO^+ beam. By observing the dissociation products produced by these states for a variety of ion source conditions, we were able to identify operating parameters for the electron-impact ion source that allowed the preparation of ground state NO^+ with either <5% population in excited vibrational levels, or with varying degrees of vibrational excitation. Our observations of facile vibrational quenching of NO^+ by low energy collisions with NO gas greatly conflict with a rate constant for this process reported by Bien,[13] who estimated the quenching to proceed 10^3 times slower than is presently observed!

We also investigated the state distribution produced in NO^+ formed by electron-impact ionization of n-Butyl nitrite, which was thought[14] to be a good source of ground state NO^+. We were able to show that although a larger fraction of ground state NO^+ is produced by this scheme, compared to that formed by ionization of NO, substantial electronic and vibrational excitation is present in the NO^+ ions.

Our measurements provide clear evidence for the predissociation of $v = 4$ in the $A^2\Sigma^+$ state, which was thought to be undissociated on the basis of lifetime measurements. Tsukiyama et al.[15] attributed their observed decrease in A state lifetime (from the $v = 3$ to $v = 4$ levels) to a strong dependence of the A-X transition moment on internuclear distance. On the basis of our observations and the recent calculations of Sheehy et al.,[16] who find little dependence of the transition moment on internuclear distance, we can derive that the A(4) level is 16% predissociated. This source for dissociation is significant for the predicted destruction of NO in the atmosphere, since the A-X transition is quite strong.

(3) P. C. Cosby, J. R. Peterson, A. B. van der Kamp, and W. J. van der Zande, Dissociative Charge Transfer of $O_2^+(v = 0)$ in Cs(6s) and Cs(6p), J. Chem. Phys. (in preparation).

This study was undertaken to establish operating conditions for the ion source that allowed the preparation of an O_2^+ ion beam with a selected degree of vibrational excitation and the absence of electronic excitation. Figure 1 of Appendix C shows that both the vibrational excitation in the ground electronic state and the large population (50%) in the long-lived $a^4\Pi_u$ excited state can be removed by allowing quenching collisions within the ion source. The small population of a state remaining at the highest pressure shown in Figure 1 is removed by lowering the electron-impact energy to 20 eV. This process yields an O_2^+ ion beam with >97% of its population in the $X^2\Pi_g(v = 0)$ level.

Despite the fact that the dissociative charge transfer spectrum of O_2^+ was thought to be well understood, our ability to produce a fully quenched beam revealed a series of features that were assigned to nonresonant production of the $3p\sigma_u$, $3p\pi_u$, and $3d\lambda_g$ Rydberg states. These were previously unobserved, being obscured by contributions from the vibrationally excited $3s\sigma_g$ states. We confirmed the assignments by observing near-resonant production of the 3p states in the charge transfer neutralization of O_2^+ by laser-excited Cs(6p) vapor.

The excited states of O_2 are strongly perturbed by Rydberg-valence coupling. These perturbations, together with the fact that many of the excited states are effectively continua, have impeded a detailed assignment of the O_2 vuv absorption spectrum. Because the production of the O_2 excited states in our work is made at internuclear distances relevant to the O_2^+ molecular ion and the preparation emphasizes their Rydberg character, the energetic shapes of the features differ appreciably from those observed in the vuv excitation of molecular O_2, which emphasizes the valence character of these states. We are collaborating with B. R. Lewis and S. T. Gibson[17] to incorporate our dissociative charge transfer spectra with their extensive vuv absorption and laser excitation measurements to develop a highly accurate model for the O_2 excited states.

REFERENCES

1. D. R. Bates, Planet. Space Sci. **38**, 889 (1990).
2. A. B. van der Kamp, P. C. Cosby, and W. J. van der Zande, Chem. Phys. **184**, 319 (1994).
3. A. B. van der Kamp, J. H. M. Beijersbergen, P. C. Cosby, and W. J. van der Zande, J. Phys. B **27**, 5037 (1994).
4. A. B. van der Kamp, L. D. A. Siebbeles, W. J. van der Zande, and P. C. Cosby, J. Chem. Phys. **101**, 9271 (1994).
5. V. J. Abreu, S. C. Solomon, W. E. Sharp, and P. B. Hays, J. Geophys. Res. **88**, 4140 (1983).
6. H. Takahashi, B. R. Clemesha, P. P. Batista, V. Sahai, M. A. Abdu, and P. Muralikrishna, Planet. Space Sci. **38**, 547 (1990).
7. R. R. O'Neil, E. T. Lee, and E. R. Huppi, J. Geophys. Res. **845**, 823 (1979).
8. E. C. Zipf, Planet. Space Sci. **36**, 621 (1988).
9. J. L. Queffelec, B. R. Rowe, F. Vallee, J. C. Gomet, and M. Morlais, J. Chem. Phys. **91**, 5335 (1989).
10. S. L. Guberman, Nature **327**, 408 (1987); Planet. Space Sci. **36**, 47 (1988).
11. S. L. Guberman and A. Giusti-Suzor, J. Chem. Phys. **95**, 2602 (1991).
12. J. -H. Yee, V. J. Abreu, and W. B. Colwell, "Aeronomical Determinations of the Quantum Yields of $O(^1S)$ from Dissociative Recombination" in *Dissociative Recombination: Theory, Experiment, and Applications*, edited by J. B. A. Mitchell and S. L. Guberman (World Scientific, Singapore, 1989).
13. F. Bien, J. Chem. Phys. **69**, 2631 (1978).
14. J. E. Thean and R. H. Johnson, Int. J. Mass Spectrom. Ion Phys. **11**, 197 (1973).
15. K. Tsukiyama, T. Munakata, M. Tsukakoshi, and T. Kasuya, Chem. Phys. **121**, 55 (1988).
16. J. A. Sheehy, C. W. Bauschlicher, S. R. Langhoff, and H. Partridge, Chem. Phys. Letters **225**, 221 (1994).
17. See for example, B. R. Lewis, J. P. England, R. J. Winkel, Jr., S. S. Banerjee, P. M Dooley, S. T. Gibson, and K.G.H. Baldwin, Phys. Rev. A 52, 2717 (1995).

APPENDIX A

ON THE BRANCHING IN DISSOCIATIVE RECOMBINATION OF O_2^+

ON THE BRANCHING IN DISSOCIATIVE RECOMBINATION OF O_2^+

H. Helm,* I. Hazell,† C. W. Walter,‡ and P. C. Cosby

Molecular Physics Laboratory
SRI International
Menlo Park, CA 94025

ABSTRACT

The product branching in dissociation of Rydberg molecules of O_2 is measured by monitoring the spatial and temporal distribution of the dissociation fragments O + O. The yield of the product states $O(^1S)$, $O(^1D)$, and $O(^3P)$ is directly determined in this experiment. The dissociation process is induced by Stark mixing of the Rydberg states with continuum valence states, as the molecules are exposed to a transient electric field in the vicinity of a metal surface. The dissociation paths open to the Rydberg states are equivalent to those open to O_2^+ ions recombining with low energy electrons. Our measurement is the first vibrationally resolved experimental determination of the branching of Rydberg states at energies in the vicinity and above the ionization threshold of O_2.

* Present Address: Fakultät für Physik, Albert-Ludwigs Universitat, 79104 Freiburg, Germany.
† Permanent Address: Institute of Physics, University of Aarhus, DK-8000 Aarhus C, Denmark.
‡ Present Address: Department of Physics and Astronomy, Denison University, Granville, OH 43023.

INTRODUCTION AND EXPERIMENT

We report observations of electric field induced predissociation of O_2 Rydberg states that lie below the lowest ionization threshold v+ = 0 of $O_2^+(X^2\Pi_g)$, as well as for Rydberg states belonging to vibrationally excited levels that lie energetically in the autoionization continuum (but are stable on the time scale of microseconds before they approach the metal surface). Figure 1 shows a schematic potential energy diagram indicating the position of the Rydberg states investigated. The neutral molecules are prepared by near resonant charge transfer of mass selected O_2^+ ions in cesium. Long lived neutral molecules are selected by time-of-flight and they are later dissociated by electric fields that the molecules experience in the vicinity of a metal surface. The vibrational dependence of the predissociation branching among the available dissociation limits of O_2 is investigated and we discuss the significance of our measurements for the branching for dissociative recombination of O_2^+ with slow electrons. The apparatus used in the present investigation is essentially identical to that used in previous work[1-7] with one minor exception that will be detailed below. Following a total flight distance of 250 cm from the electron impact ion source, the O_2^+ beam passes through a cell of Cs vapor (see Fig. 2). A small fraction (<<1%) of the O_2^+ beam is neutralized in the Cs vapor, and the residual charged particles leaving the cell are swept out of the beam by deflection plates 26 cm downstream from the cell. Neutral particles travel unimpeded from the cell to a circular aperture (diameter 3 mm) and to a slit assembly (54 cm from the charge transfer cell). The slit, fabricated from razor blades with a nominal radius of curvature of order 1 μm, provides an opening of dimension 10 mm x 0.3 mm. All undissociated particles passing through the open area of the slit are collected by a 50 mm x 1.27 mm beam flag positioned 10 cm downstream from the slit. If a molecule dissociates in the region between the slit and the beam flag and its fragments escape collection by the beam flag, these fragments travel a distance L ~ 100 cm to a position-sensitive detector for correlated fragments. The detector explicitly measures the spatial (R) and temporal (Δt) separations of the two correlated fragments produced by the dissociation of a single molecule of mass M, energy E_0, and velocity v ($E_0 = Mv_0^2 / 2$) to define the center of mass translational energy (W) released in the dissociation:[1,8]

$$W = \frac{E_0}{4L^2}(R^2 + v_0^2\Delta t^2). \qquad (1)$$

The combination of the narrow slit and the beam flag geometrically defines a range of distances from the detector, L, for which the two correlated fragments can be both produced and detected. The narrow slit (110.8 cm from the detector) defines the maximum value for L; the

beam flag (100.8 cm from the detector) defines the minimum value for L. The effect of an indeterminacy in L, $\Delta L \leq 10$ cm, is to produce a broadening in the W release values calculated from the fragment temporal and spatial separations, $\Delta W/W = 2\Delta L/L$. If unimolecular dissociation occurs with equal probability over the full range of the interaction region ($\Delta L \sim 10$ cm), the resolution is quite poor with $\Delta W/W = 0.18$. In contrast, prompt dissociation of a single molecular energy level prepared by photoexcitation within a ~2 mm laser beam diameter is found to yield $\Delta W/W = 0.015$.[3] The narrow energy release spectra observed in our experiment show that dissociation occurs promptly, only in the vicinity of the slit assembly.

OBSERVATIONS

Following formation of excited O2* molecules by the reaction

$$O_2^{\dagger} + Cs \rightarrow O_2^{*} + Cs^{+}, \tag{2a}$$

a very weak dissociation signal (1 in 10^8 $O_2^{\dagger}$ ions) is observed following passage of the molecules through the slit assembly:

$$O_2^{*} \rightarrow O + O + W, \tag{2b}$$

where W is the released translational energy. A typical distribution of energy releases observed in this dissociation is shown in Figure 3. The spectrum in Fig. 3 is a histogram of the number of detected pairs of correlated fragments (fragment intensity) yielding a given value of energy release W [Eqn. (1)] in the range $0.5 \text{ eV} \leq W \leq 8.5 \text{ eV}$. Both spectra have been corrected for the variation of the collection efficiency with energy release.[7]

The ratio of the fragment positions for each correlated dissociation pair relative to the center of the detector is found to be peaked at unity. This is consistent with the dissociation products being of equal mass, as expected for fragmentation from O_2 molecules. In addition, the degree of correlation in the spatial and temporal separations of the dissociation fragments proves that the signal in Fig. 3 does not arise from grazing collisions of the molecules with the surface of the slit.

The energy release peaks in Fig. 3 fall into four groups, each containing 6 or 7 peaks of significant intensity. The energy release values corresponding to the midpoint of each peak are given in Table I. Within the experimental uncertainty (±10 meV), the spacings of the peaks within

each group is identical and these spacings correspond to those[9,10] of the vibrational levels v=0-6 of the O_2^+ $X^2\Pi_g$ state.

The observed fragmentation arises from dissociation of very high principal quantum number Rydberg states of O_2 built on the O_2^+ ($X^2\Pi_g$) core to four distinct dissociation limits, producing: $O(^1S) + O(^1D)$, $O(^1D) + O(^1D)$, $O(^1D) + O(^3P)$, and $O(^3P) + O(^3P)$. The energy assignment also identifies the vibrational quantum number of the ionic core as labelled in Fig. 3.

Dissociation is also observed with an electrostatic potential difference applied between the two razor blades. Figure 4 shows the energy release spectra observed at five nominal values of the electric field. Each of the spectra in this figure is approximately normalized to the same beam flux and accumulation time to allow comparison. It can be seen that the external field affects the widths, relative intensities, and nominal values of the energy releases in the spectra. The relative intensity of the v=0 peaks increases increases with applied field up to approximately 20 V (~600 V/cm), whereas the intensities for $v > 0$ decrease rapidly. The reason for the increase in the signal originating from Rydberg molecules in $v = 0$ is that dissociation due to the external electric field contributes under these conditions. For Rydberg molecules with $v > 0$, the external field has an adverse effect: it more efficiently induces autoionization than dissociation. Consistent with this explanation, we observe that the peaks corresponding to $v = 0$ appreciably broaden to lower W with applied field, indicating that increasingly lower Rydberg levels are affected by the field-induced dissociation process. The positions of the peaks within each group shift slightly to lower values of W with applied field, consistent with the effect of lowering the dissociation and autoionization threshold with increasing external field.

In the present experiment, the state distribution in the precursor O_2^+ beam was controlled by adjusting the ion source pressure and residence times of the ions within the source. The actual electronic, vibrational, and rotational populations of the O_2^+ ions at the time of charge-transfer neutralization were explicitly determined by observing the products produced by dissociative charge transfer. The results were fully consistent with the earlier work of Walter et al.[6] and of van der Zande et al.[11] Briefly, production of the O_2^+ beam at high O_2 source pressure and long source residence times yielded an ion beam with >95% population in the first several vibrational levels of the $X^2\Pi_g$ state. Production of the beam at low source pressures and short residence times produced comparable populations in the $X^2\Pi_g$ and $a^4\Pi_u$ states, with the population of the latter extending to v>14. The dissociating molecules were only found in beams containing the $a^4\Pi_u$ state. This unambiguously identifies the electronic state of the O_2^+ parent of the dissociative Rydberg atoms (reaction 2a) to be the $a^4\Pi_u$.

DISCUSSION

NATURE OF THE DISSOCIATING STATES

Clues to the nature of the dissociating states are found in several aspects of the observed fragment energy release spectra, including the energies and widths of the peaks, and the changes induced by the applied electric field. The potential energy of the dissociating state (E_{tot}) is released as kinetic (W) and potential (E_{int}) energy of its dissociation products at infinite separation, $E_{tot} = E_{int} + W$.

In the present experiment, the translational energy spectrum of the fragments specifically measures only the kinetic energy component, W. However, the possible internal energy states in the product atoms are relatively few and are widely separated in energy. The separations among the four groups of peaks observed in the translational energy release spectrum of the O_2 molecule match the energy separations of the various O_2 dissociation limits, hence a unique assignment of the dissociation products can be made. The electronic states of the product O atoms are identified in Fig. 3 and in Table I. We note first that each group contains discrete peaks spaced by roughly 0.23 eV, the vibrational spacing of the $O_2^+ X^2\Pi_g$ state. Assigning the vibrational numbering of the peaks as given in Table I, i.e. with the lowest member of each group assigned as v=0, and taking $W_{obs} = W$, the values of E_{level} for the four groups of peaks are found to be: 6.951±0.017 eV for $O(^1S) + O(^1D)$, 6.973±0.008 eV for $O(^1D) + O(^1D)$, 6.970±0.012 eV for $O(^1D) + O(^3P)$, and 6.953±0.008 eV for $O(^3P) + O(^3P)$. The four values are reasonably consistent and yield an energy for v=0 of the dissociating state of 6.963 ± 0.004 eV above the ground state atom limit. For comparison, the lowest level of the $O_2^+ X^2\Pi_g(v=0)$ lies at 6.954 ± 0.001 eV. Thus, the dissociating states must lie very close to the ionization limit of the molecule, as indicated in Fig. 1.

To further characterize the nature of the dissociating states, we turn now to the widths of the translational energy peaks. In simulation of the energy release spectra, we found that the observed broadness of the peaks is due to an initial population of a range of internal energy levels of the Rydberg molecules (rotational and fine-structure) and to the presence of molecules in a range of values of n. Since the dissociating levels are very high Rydberg states of O_2, an internal structure very nearly that of the $O_2^+ X^2\Pi_g$ state could be expected, i.e. a spin-orbit splitting of order 0.025 eV and a rotational manifold described by the rotational constants of the ion. Based on these considerations, the experimental spectra were fit presuming the dissociation of 7 vibrational levels in a single Rydberg state of O_2 with internal energy levels exactly described by the $O_2^+ X^2\Pi_g$ molecular constants, together with an apparatus function characteristic of the present experimental arrangement. We further presumed that both spin-orbit components have equal populations and

dissociation rates, that the rotational population distribution in all vibrational levels can be characterized by a single Boltzmann temperature (T_{rot}), ^3P_J dissociation products in a statistical distribution, and that the dissociations occur within a region of length ΔL centered at the slit.

The spectra were found to be well described by a single rotational temperature T_{rot} = 630±50K, comparable to the value observed by Walter et al.[17] Also, analysis of spectra recorded at 3 and 5 keV beam energy yielded the same value for the energy of the dissociating state, $E_v^+{}_{=0}$ = 6.931 ± 0.004 eV, where the error refers only to the standard deviation in the fits. This value lies 31 meV below that estimated from the Gaussian fits (Table I). This was to be expected because now the energy refers to the lowest energy level rather than to the peak of a rotational and spin-orbit population distribution. In comparison to the energy of $O_2^+(X^2\Pi_g)$ at 6.954 eV, $E_v^+{}_{=0}$ lies 23 meV lower in energy.

Under the assumption that $\Delta L \rightarrow 0$, the range of participating Rydberg states is essentially equal to the difference in energy between $E_v^+{=}0$ and the ionization energy of O_2, 0.023 eV, corresponding to a series of O_2 Rydberg states with quantum numbers in the range from n = 24 to the ionization limit. Obviously the range will get smaller if a finite value for ΔL is assumed. In any case, the range ΔL has to be significantly smaller than a few mm to be consistent with the observed independence of peak width with beam energy. The range of energies over which excited states participate in the dissociation process for zero field and for a potential difference of 200 V applied to the slit is indicated in Fig. 1.

DISSOCIATION PRODUCT BRANCHING

Table II gives the relative flux of fragments at each of the four dissociation limits. The data shown represent the average between the results obtained at 3 keV and at 5 keV beam energies. The distribution is dominated by the fact that the greatest flux of fragments is produced at the $O(^1D) + O(^3P)$ limit for all vibrational levels. The next higher product channel is the production of two ground state atoms, accounting for roughly 20% of the fragments, but production of $O(^1D) + O(^1D)$ is also found to be significant. The highest energy dissociation channel, $O(^1S) + O(^1D)$ is a relatively minor channel. No evidence is found for production of $O(^1S) + O(^3P)$ fragments. Thus fragments produced at this limit represent < 1% of the total product yield.

DISSOCIATION MECHANISM

It is clear from our results that the processes leading to dissociation of O_2^* must be confined to a narrow region in the vicinity of the slit assembly. We propose that the following mechanism is primarily responsible for the observed dissociation: Let us assume that a very weak channel in the

charge transfer process leads to production of $(n\ell)X^+$ Rydberg states with a wide range of values of n and ℓ. Rydberg states with low values of ℓ generally have more efficient coupling to the valence continuum states. Hence, these lower ℓ members of the O_2^* ensemble of states will be removed from the beam during the transit period to the slit assembly by predissociation and by radiative decay. Thus at the slit, only a small concentration of O_2^* will remain undissociated, and these will consist primarily of high ℓ and high n Rydberg states. In the immediate vicinity of the slit, the O2* beam is subjected to sudden changes of the residual electric field. Far from the slit assembly residual fields stem from stray fields from the vacuum chamber (distance ~10 cm) and the motional electric field (~10 mV/cm for a 5 keV beam) due to the uncompensated earth's magnetic field. The sudden change in stray fields in the vicinity of the slit will lead to Stark mixing of the $n\ell$ states, thereby admixing to all or some of the high ℓ quantum levels components of the lower ℓ states that are effectively predissociated by the valence continuum states.

The high n Rydberg states are also subject to field-induced ionization and the Stark mixing can increase the rate of autoionization of Rydberg states with $v > 0$. Since only correlated pairs of *neutral* fragments are detected in the present experiments, the effect of O_2^* ionization is to remove molecules from contributing to the dissociation flux. This process is evident from the observed dependence of the flux of dissociating molecules on the magnitude of the electric field applied across the slit, and from the observation that the $v = 0$ peaks broaden to lower energy release with applied field, whereas $v > 0$ peaks do not perceptibly broaden, but only shift to lower values of energy release.

RELATIONSHIP TO DISSOCIATIVE RECOMBINATION

The variation of the predissociation branching with vibrational level reflects the availability of the different continuum states of O_2 to which the O_2^+ core + Rydberg electron can couple, as well as the dynamics of the dissociating system as it experiences the molecular continuum. In this sense, the dissociative process investigated here is intimately related to the molecular dynamics involved in dissociative recombination (DR) of O_2^+ with electrons, both in the direct as well as in the indirect DR channel.[12] Therefore, our results can answer the important question of which final atomic states are produced when a specific vibrational level of superexcited oxygen molecule predissociates.

Previous investigations of O_2^+ DR were primarily concerned with the rate of formation of $O(^1S)$, the origin for the green atomic oxygen emission in the night sky.[13] Theory[14] predicts a yield of $O(^1S)$ (relative to a yield of 2 for all atoms) of 0.0024 for $v^+=0$, 0.051 for $v^+=1$, and 0.15 for $v^+=2$. This vibrational sensitivity is primarily a consequence of the location of the continuum state that is expected to contribute most strongly to the dissociative recombination reaction.

Generally higher yields are deduced from satellite based observations,[15] which also predict an increase in the yield with vibrational quantum number. By comparison, our experimental yields for $O(^1S)$ shown in Table II increase only slightly for v = 0-2 and actually decrease for the higher vibrational levels, in marked contrast to the vibrational dependence that is currently accepted. On the other hand, our experimental yields for $O(^1D)$ range from 0.73 to 0.82 in the lowest seven vibrational levels. Previous laboratory and satellite-based observations place this yield near unity,[15] consistent with our more precise branching values. Queffelec et al.[16] have determined quantum yields in dissociative recombination of vibrationally hot oxygen molecular ions. Their results of 0.44 for $O(^1S)$ and 0.96 for $O(^1D)$ are higher than the results of the present study.

ACKNOWLEDGEMENTS

This research was supported by Grant No. NAGW-360 from the NASA Space Sciences Branch. H. H. acknowledges partial support by the Deutsche Forschungsgemeinschaft through SFB 276, TP C13.

REFERENCES

1. H. Helm and P. C. Cosby, J. Chem. Phys. **86**, 6813 (1987).
2. P. C. Cosby and H. Helm, Phys. Rev. Lett. **61**, 298 (1988).
3. P. C. Cosby and H. Helm, J. Chem. Phys.**90**, 1434 (1989).
4. H. Helm and P. C. Cosby, J. Chem. Phys. **90**, 4208 (1989).
5. C. Bordas, P. C. Cosby, and H. Helm, J. Chem. Phys. **93**, 6303 (1990).
6. C. W. Walter, P. C. Cosby, and J. R. Peterson, J. Chem. Phys. **98**, 2860 (1993).
7. P. C. Cosby, J. Chem. Phys. **98**, 7804 (1993).
8. D. P. de Bruijn and J. Los, Rev. Sci. Instrum. **53**, 1020 (1982).
9. P. H. Krupenie, J. Phys. Chem. Ref. Data **1**, 423 (1972).
10. R. R. Laher and F. R. Gilmore, J. Phys. Chem. Ref. Data **20**, 685 (1991).
11. W. J. van der Zande, W. Koot, J. R. Peterson, and J. Los, Chem. Phys. **126**, 169 (1989).
12. J. N. Bardsley, J. Phys. B. **1**, 349 (1968).
13. D. R. Bates, Planet. Space Sci. **38**, 889 (1990).
14. S. L. Guberman and A. Giusti-Suzor, J. Chem. Phys. **95**, 2602 (1991).
15. J. -H. Yee, V. J. Abreu, and W. B. Colwell, "Aeronomical Determinations of the Quantum Yields of $O(^1S)$ from Dissociative Recombination" in *Dissociative Recombination: Theory, Experiment, and Applications*, edited by J. B. A. Mitchell and S. L. Guberman (World Scientific, Singapore, 1989).
16. J. L. Queffelec, B. R. Rowe, F. Vallée, J. C. Gomet, and M. Morlais, J. Chem. Phys. **91**, 5335 (1989).

FIGURE CAPTIONS

1. Location of the excited states of molecular oxygen that participate in the observed dissociation process, relative to the lowest vibrational levels of the molecular ion. The potential energy curve of one of the continuum states in this energy region is indicated by the dashed curve.

2. Schematic of the fast beam apparatus. Excited molecules, produced by charge transfer in cesium vapor, are observed to dissociate in the immediate vicinity of the slit, both in the presence and absence of an electric field applied externally across the slit. The correlated neutral dissociation products are monitored on the position and time-sensitive detector. The position of the laser beam, used to calibrate the detector, is also shown.

3. Measured energy release distribution for correlated oxygen atoms formed by dissociation at the slit in the absence of an external applied electric field. The energy states of the oxygen atom products and vibrational quantum numbers of the dissociating O_2 Rydberg states are indicated in the figure.

4. Variation in the distribution of energy releases as a function of the voltage applied to the slit.

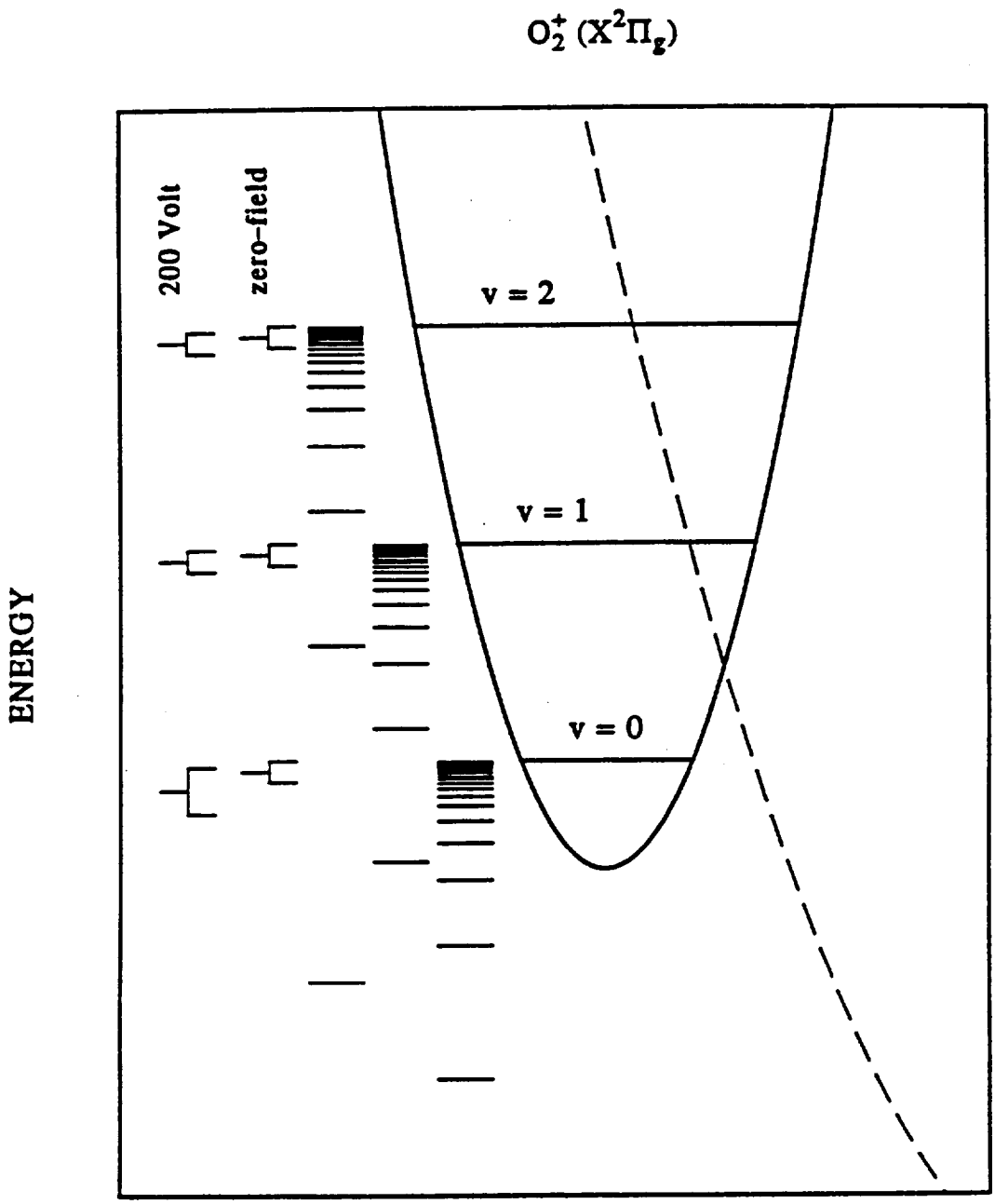

PREDISSOCIATION OF RYDBERG STATES OF O_2

Figure 1

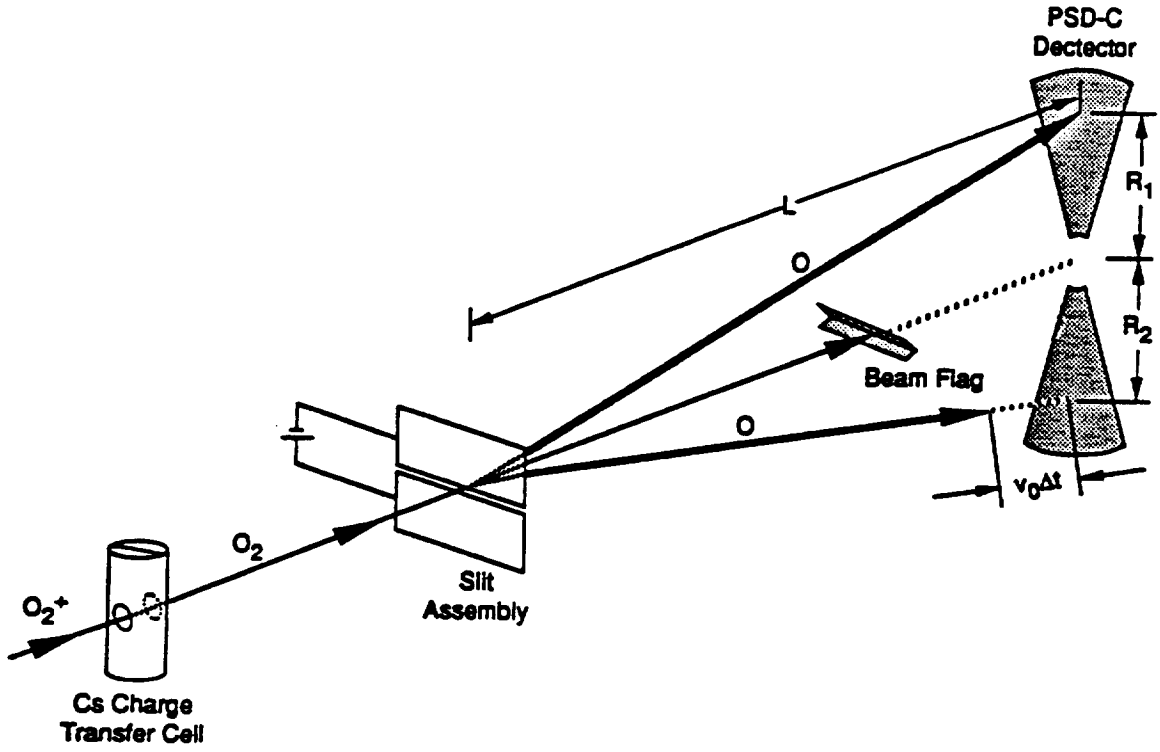
PSD-C
Dectector
L
O
R1
R2
Beam Flag
O
v0Δt
O2
O2+
Slit
Assembly
Cs Charge
Transfer Cell

Figure 2

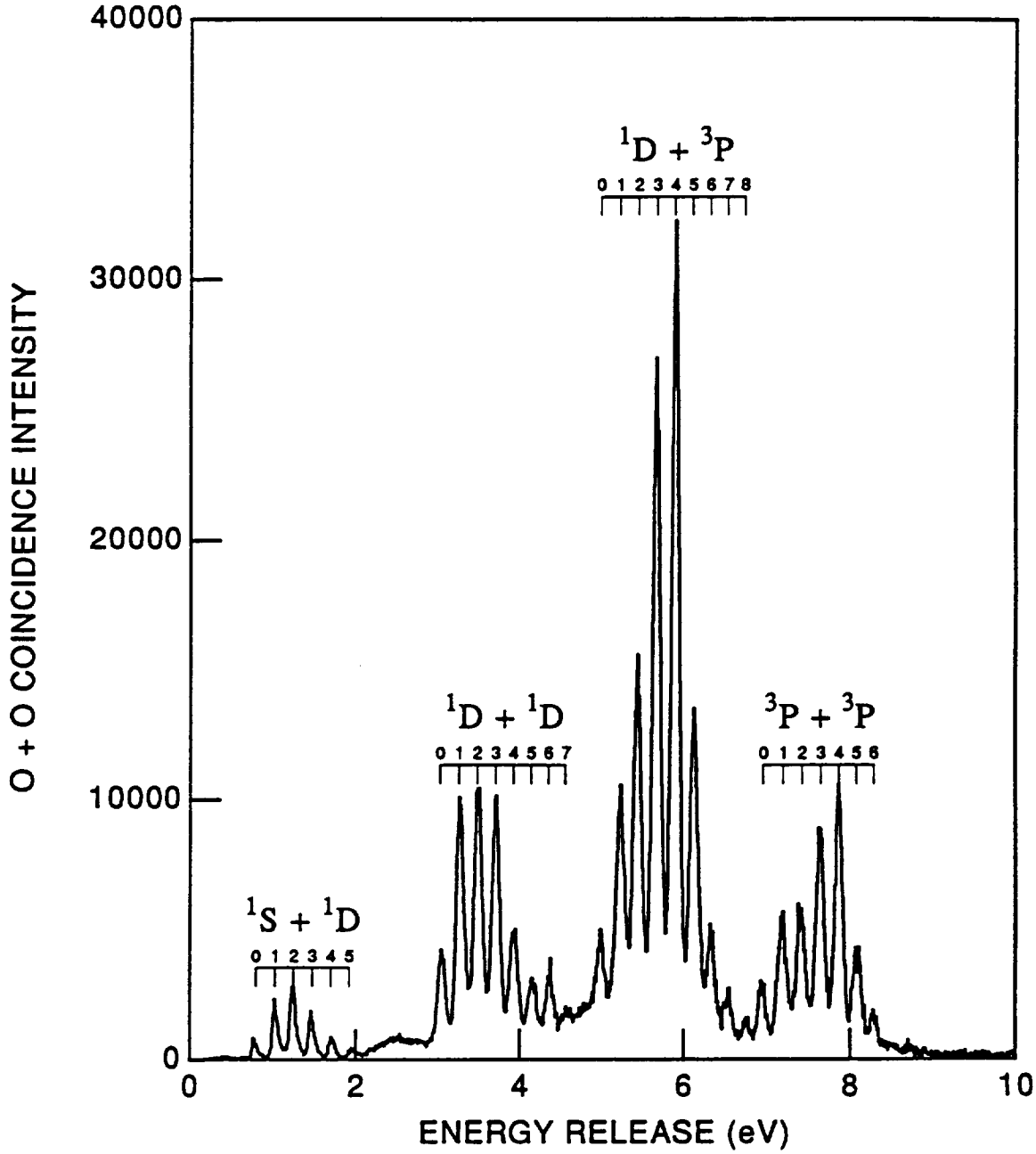
40000
30000
20000
10000
0
O + O COINCIDENCE INTENSITY
$^1D + {}^3P$
0 1 2 3 4 5 6 7 8
$^1D + {}^1D$
0 1 2 3 4 5 6 7
$^3P + {}^3P$
0 1 2 3 4 5 6
$^1S + {}^1D$
0 1 2 3 4 5
0
2
4
6
8
10
ENERGY RELEASE (eV)

Figure 3

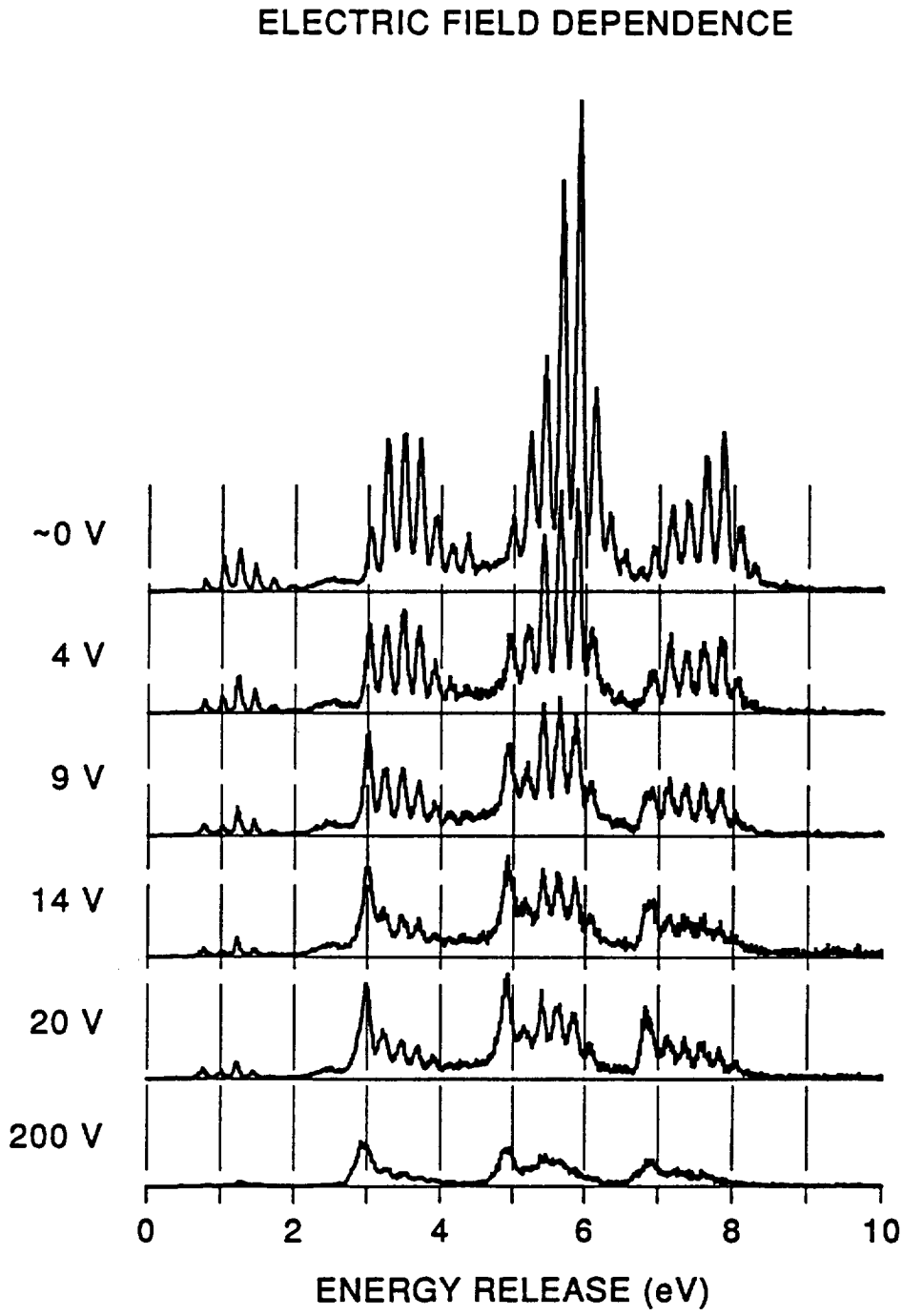
ELECTRIC FIELD DEPENDENCE
~0 V
4 V
9 V
14 V
20 V
200 V
0
2
4
6
8
10
ENERGY RELEASE (eV)

Figure 4

Table I. Observed translational energy releases (W_{obs}) of peaks in the O_2 dissociation spectrum. Peaks are fitted as Gaussians and W refers to the centroid of the Gaussian. The upper and lower entries for each vibrational level refer to data obtained with a 3 keV and 5 keV O_2 beam energy, respectively. Deviations, W_{obs}-W_c, are referenced to a calculated value for the translational energy release W_c that assumes a single dissociating state at the ionization limit (IP = 6.954 eV) with vibrational energies G_v.

v	$O(^1S) + O(^1D)$		$O(^1D) + O(^1D)$		$O(^1D) + O(^3P)$		$O(^3P) + O(^3P)$		G_v (eV)
	W_{obs} (eV)	W_{obs}-W_c (meV)	W_{obs} (eV)	W_{obs}-W_c (meV)	W_{obs} (eV)	W_{obs}-W_c (meV)	W_{obs} (eV)	W_{obs}-W_c (meV)	
0	0.790	-7	3.047	28	5.001	14	6.939	-15	0.
	0.761[a]	(-36)	3.027	8	5.029[a]	(42)	6.944	-11	
1	1.044	15	3.270	18	5.235	16	7.178	-8	0.2322
	1.027	-2	3.281	29	5.258	39	7.189	-3	
2	1.261	3	3.498	18	5.446	-1	7.408	-6	0.4604
	1.243	-14	3.505	25	5.449	2	7.417	3	
3	1.481	0	3.713	9	5.675	49	7.635	-4	0.6845
	1.457	-24	3.725	21	5.680	23	7.646	7	
4	1.727	26	3.931	8	5.901	10	7.861	2	0.9045
	1.700	-11	3.949	25	5.914	34	7.862	3	
5	1.964	(46)	4.161	21	6.124	17	8.088	13	1.1206
	1.925	7	4.193[a]	(53)	6.141		8.043[a]	(-32)	

[a]Weak or blended feature.

Table II. Comparison of oxygen atom quantum yields determined in this work with theoretical results (Ref. 14) and observational estimates from satellite observations (Ref. 15).

	$O(^1S)$		$O(^1D)$		$O(^3P)$	
v	Ref. 14	This Work	Ref. 15	This Work	Ref. 14	This Work
0	0.0024	0.033	~1	0.73	~1	1.24
1	0.0051	0.041	~1	0.79	~1	1.17
2	0.150	0.045	~1	0.83	~1	1.13
3	--	0.018	~1	0.81	~1	1.17
4	--	0.010	~1	0.78	~1	1.21
5	--	0.015	~1	0.82	~1	1.16
6	--	0.007	~1	0.78	~1	1.21

APPENDIX B

DISSOCIATIVE CHARGE-TRANSFER OF NO^+

DISSOCIATIVE CHARGE-TRANSFER OF NO^+

P. C. Cosby
Molecular Physics Laboratory
SRI International
Menlo Park, CA 94025

A. Barbara van der Kamp and Wim J. van der Zande
FOM-Institute for Atomic and Molecular Physics
Kruislaan 407
1098 SJ Amsterdam, The Netherlands

ABSTRACT

Predissociated n=3 Rydberg states of NO, formed by charge transfer neutralization of NO^+ in Cs vapor at energies in the range of 3-5 keV, are observed by translational spectroscopy of their dissociation products. The $(3p\sigma)X^+ C^2\Pi$ and $(3p\pi)X^+ D^2\Sigma^+$ states are observed in their ground vibrational levels with rotational resolution. Higher vibrational levels of these states are observed and the v=4 level of the $(3s\sigma)$ $A^2\Sigma^+$ is found to dissociate, in contrast to recent conclusions based on emission lifetimes. The rovibrational distributions observed in these Rydberg states are used to monitor the state composition of the NO^+ ion beam under a variety of ion source conditions. Vibrational quenching of NO^+ by NO is found to be rapid at near-thermal collision energies, with a quenching rate constant $\sim 10^{-10}$ cm^3/s, in contrast to early estimates for this rate constant that were three orders of magnitude smaller. A large number of Rydberg states converging to excited electronic states of NO^+ are also observed to be produced in the charge transfer under conditions where NO^+ excited states were expected to be present in the reactant ion beam.

INTRODUCTION

The NO^+ ion is characterized both by having an unusually low ionization energy (9.25 eV) and by having a very large number of metastable excited states in the singlet, triplet, and quintet manifolds that lie at energies 5-13 eV above the ground electronic state.[1,2] These excited states are copiously produced by direct ionization from ground state NO[3,4] and a large number of the states are long-lived[2,5,6] on time scales ~10^{-4} s. The effects of these long-lived states have been noted in early studies of ion molecule reactions[7] and of collision-induced dissociation[8,9] by beam techniques. Mathis et al.[10] have estimated that 47% of an ion beam created by 100 eV electron impact on NO gas at low pressure is in long-lived electronically excited states. Rate constants have been measured for the quenching of NO^+ states and are found to be quite large for the reaction of the lowest excited state, $a^3\Sigma^+$, with NO at thermal energies (5×10^{-10} cm^3/s),[11,12] but are potentially much smaller for the higher energy states.[13]

An additional characteristic of NO^+ is that substantial vibrational excitation is produced in the ground electronic state even by direct ionization due to the large difference in equilibrium internuclear distances of the neutral and ion. Bien[14] has measured the vibrational quenching rate for NO^+ $X^1\Sigma^+(v=1,2)$ state to be small in N_2 gas (2×10^{-12} cm^3/s) and has estimated from his measurements that the rate is yet smaller ($1.5\times10^{-13\pm0.5}$ cm^3/s) in NO gas. These small rates suggest that the production of a relaxed, ground state NO^+ ion beam would be difficult, if not impossible. The purpose of the present work is to apply the techniques of dissociative charge transfer in cesium vapor and translational spectroscopy to identify predissociated Rydberg states of NO and use the production of these states to assay the electronic and rovibrational state composition of the NO^+ ion beam produced under a variety of electron-impact ionization conditions.

EXPERIMENT

The basic experimental strategy for determining the electronic and rovibrational distributions in the NO^+ ion beam is to measure the translational energies released to the N + O atom products following dissociative charge transfer (DCT) of NO^+ + Cs:

$$NO^+(i,v_i) + Cs \rightarrow NO^*(n,v_n) + Cs^+ \quad (1a)$$

$$NO^*(n,v_n) \rightarrow N(^4S) + O(^3P) + W(n,v_n), \quad (1b)$$

where i and v_i denote the initial electronic state and vibrational level of the NO^+ reactant and n and v_n denote the electronic state and vibrational level of the excited neutral state NO^*, and $W(n,v_n)$ denotes the translational energy released to the atomic products.

The use of Cs as the electron donor in Reaction (1a) offers two distinct advantages for monitoring the ion beam state distribution. First, the 3.89 eV ionization potential of Cs is close to those of the lowest Rydberg states (n = 3) of most simple molecules, thus the electron capture is nearly resonant (negligible change in electron energy) for the formation of these states on the initial ion core. This aspect and the large radius of the outer electron in Cs permits long range transfer with large ($100 Å^2$) cross sections[15] and little or no momentum transfer to the nuclei. Second, the Rydberg state, which consists of an ion core with a loosely bound electron, has a molecular potential energy curve that is very similar to that of the parent ion. Thus the Franck-Condon matrix governing the vibrational transitions in the electron capture transition is nearly diagonal, $|<\Psi_{v_i}|\Psi_{v_n}>|^2 \sim \delta_{v_i,v_n}$, and the distribution of v_i in the initial ion is closely reproduced in the v_n distribution of the Rydberg product state. Rotational transitions are also quite weak in the long range transfer.[16] Finally, the lowest Rydberg states generally lie higher in energy than the lowest dissociation limit of the molecule. Imbedded in the continua of a variety of valence electronic states and with generally slow rates for spontaneous photon emission, the usual fate of the Rydberg states is predissociation, Reaction (1b). Through conservation of energy, this allows Rydberg state rovibrational levels, which are characterized by discrete values of molecular *potential* energy, $E(n,v_n)$, to be viewed as atomic dissociation products that are characterized by discrete values of (center-of-mass) *kinetic* energy, $W(n,v_n)$, and potential energy of the atoms, E_{atoms}:

$$E(n,v_n) = D_0^0 + W(n,v_n) + E_{atoms}, \qquad (2)$$

where D_0^0 is the dissociation energy of NO (6.4968 eV).[17] Reaction (1b) has been written for the production of ground state atoms ($E_{atoms} = 0$), which is the only open product channel for the $NO^+(X^1\Sigma_g^+)$ ions. For NO^+ ions in electronically excited states, the production of one or more excited atoms is energetically allowed and E_{atoms} represents the sum of the atomic excitation energies.

The combination of these three characteristics of DCT in Cs allows a reliable mapping of the relative rovibrational population distribution in the molecular ion beam into a relative flux distribution in the translational energy spectrum of the atomic dissociation products. This behavior has been demonstrated for $H_2^+(X^2\Sigma_g^+)$,[18,19] $O_2^+(X^2\Pi_g)$,[20-23] $O_2^+(a^4\Pi_u)$,[24] and HeH^+ reactants[25] and it can be anticipated that it also holds for NO^+.

Translational Spectroscopy

The apparatus used in the present experiments has been described previously[23] and will only briefly be discussed here. A beam of NO^+ ions is formed in an electron impact ion source, accelerated to a selected energy in the range of 3-6 keV, mass selected, and collimated to ~2 mrad angular divergence by a series of apertures. This collimated NO^+ beam then passes through a heated, stainless steel charge-transfer cell containing Cs vapor The neutralization region of the oven is nominally defined by 1 mm diameter entrance and exit apertures separated by 5 mm, but the effective length is found to be approximately twice this distance, presumably due to Cs vapor confined by the surrounding heat shields. The Cs vapor density is regulated by controlling the temperature of the cell. For the experiments described here, a selected oven temperature in the range of 65-90C provided an adequate Cs pressure ($\sim 1 \times 10^{-4}$ Torr) to produce a copious DCT fragment flux with negligible attenuation of the NO^+ ion beam. Beyond the immediate region of the charge transfer oven, the apparatus was maintained at a pressure $< 2 \times 10^{-7}$ Torr.

Charged particles exiting the oven are swept out of the beam by a weak electric field and collected. Collimated fast neutrals leaving the oven are collected by a narrow beam flag positioned either 34 cm or 63 cm downstream of the oven. If an NO^+ ion captures an electron from the Cs to form a dissociative state of NO and the two fragments from this dissociative state are produced with sufficient velocity perpendicular to the direction of beam propagation to escape collection by the beam flag, this pair of neutral fragments travels an additional distance to a position- and time-sensitive detector for correlated fragments (PSD-C).[26] It explicitly measures the arrival time difference $\Delta t = t_2 - t_1$ of the two fragments produced in the dissociation of a single molecule as well as the radial distance of each fragment's impact on the detector, (R_1, R_2), relative to the incident beam axis. Knowing the distance L from the point of molecular dissociation (the charge transfer oven) to the detector, the initial translational energy E_0 of the beam ($E_0 = Mv_0^2/2$, where $M = m_1 + m_2$ and v_0 are the mass and initial velocity of NO^+), and the measured temporal (Δt) and spatial ($R = R_1 + R_2$) separations of the fragments at the detector define the total center-of-mass energy release (W):[27]

$$W = E_0 \frac{m_1 m_2}{M^2} \frac{R^2 + (v_0 \Delta t)^2}{L_0^2} \left(1 - 2\frac{v_0 \Delta t}{L_0} \frac{|m_2 - m_1|}{M}\right) \qquad (3)$$

The ratio Z

$$Z \equiv \frac{R_1}{R_2}\left(1-\frac{v_0 \Delta t}{L_0}\right) \approx \frac{m_2}{m_1} \tag{4}$$

allows us to determine the fragment masses m_1 and m_2 from the known mass M of the parent molecule.

For a PSD-C detector of infinite dimensions, the Jacobian for the transformation from the center-of-mass frame of the dissociating molecule to the laboratory frame of the detector is unity.[27] However, the practical dimensions of the detector require that 0.7 cm $\leq R_1, R_2 \leq$ 3.5 cm. This restriction on the allowed range of fragment radial separation introduces a W dependence to the collection efficiency of the fragments This variation in efficiency is calculated from a Monte Carlo simulation of the dissociation fragment trajectories within the physical dimensions of the apparatus. Fragment spectra shown herein have been corrected for this efficiency. The dimensional restrictions of the detector also set a definite limit on the minimum energy release W_{min} that can be observed for a given beam energy E_0 and distance L, where the separation of the fragments is insufficient for both fragments to strike active areas of the detector. Two configurations were used for the present experiments that allowed flight distances L of either 164 cm or 260 cm, the latter used to examine processes leading to small energy releases (W_{min} ~ 0.05 eV).

Ion Source

A Nier-type electron impact ion source is used in the present studies. Its active geometry is a short cylinder of 20 mm diameter and 5 mm length. Electrons from an external, directly-heated ThO_2 coated irridium filament are accelerated to their desired energy, pass through a 1mm x 2 mm slit in the cylindrical wall, and are collected on a "trap" plate mounted within the source at the opposite wall. A weak (~100 gauss) magnetic field provides some collimation of the electron beam between the filament and the trap. One end of the source has a 1 mm diameter ion exit aperture on the cylinder axis and the other is formed by a pair of half-circular repeller plates of 15 mm diameter located 5 mm from the exit aperture and mounted on the wall that closes the cylinder. The ions are thus sampled at 90° with respect to the electron beam axis, which is midway between the exit aperture and repeller plates. The ion trajectories within the source can be controlled by potentials on the repeller plates. All source components (with the exception of the external magnet) are constructed of stainless steel and high purity alumina, with only stainless steel directly exposed to ion or electron impact.

Gas is introduced to the ion source through a stainless steel tube at a rate controlled by a leak valve. For most of the present experiments, the gas was pure (99%) nitric oxide. For one experiment, the "gas" was room-temperature vapor from a vial of n-Butyl nitrite, $CH_3(CH_2)_3ONO$ (95% purity in the liquid phase). The gas pressure in the source is measured only indirectly. Input pressure is monitored by a pirani gauge on the low pressure side of the leak valve, and gas effusing from the source is monitored by an ionization gauge on the outer vacuum chamber near the source. Calibration of these two pressure indicators in terms of gas density within the ionization volume was made using the total ionization cross sections of CO_2[28] and of O_2[29] by measuring the electron current and ion currents in the source with alternate bias voltages on the repeller plates as a function of source gas pressure for these gases. The ion gauge response was scaled for the relative ionization cross sections[30] of O_2 and NO to derive the NO gas pressure in the ion source, which is probably accurate to within a factor of two. The combination of source gas pressure, ion residence time within the source (repeller voltage), and electron ionization energy is used to control the state distribution within the NO^+ ion beam.

OBSERVATIONS AND DISCUSSION

Figure 1 shows the fragment kinetic energy release spectrum observed from the dissociative charge transfer reaction (1), where the NO^+ ions are created by electron impact on low pressure (0.1 mT) NO gas at selected electron energies. A relatively high ion source repeller voltage (20 V) was used for these spectra to minimize the source residence times of the nascent NO^+ ions.[31] At the higher electron impact energies, the DCT spectrum is rather complex and not fully identified, owing to the paucity of information[3,17,32] on the Rydberg series (both doublet and quartet states) converging to the many excited states of NO^+. However, a qualitative explanation of the spectrum can be made. The features that appear at $W > 3$ eV must arise from the production of the high energy $B^1\Pi$ and $c^3\Pi$ states by electron impact at energies > 20 eV. These states are highly populated in the ionization of NO as demonstrated by their prominence in the photoelectron spectrum.[4] Allowed radiative transitions are possible from each of these states to lower electronic states in NO^+, but the radiative lifetimes for such transitions are not known. Given that the intensity associated with these features in the DCT spectrum decreases abruptly with the decrease in nominal electron-impact energy between 30 eV and 22 eV, with no corresponding change in the DCT features at $W < 3$eV, suggests that such radiative transitions are slow relative to the ~20 μs transit time of the ions from the source to the Cs charge-transfer cell. At lower energies, seven electronic states of NO^+ lie in the region of 15.7 - 18.1 eV and are also prominent in the photoelectron spectrum. Six of these states are known[2,5] to have long radiative lifetimes (>80μs) and if formed, should participate in the dissociative charge transfer. Electron capture into

predissociated NO $3\ell\lambda$ Rydberg states built on the electron configurations of these long-lived excited ion states give rise to the features in the DCT spectrum at energy releases in the range 1 eV $\leq W \leq 3$ eV. These features change very little as the nominal electron impact energy is decreased from 100 eV to ~15 eV. Reducing the electron impact energy below the energetic threshold for creating the metastable ion states allows observation of the few low W features that can be clearly identified with DCT of $NO^+ X^1\Sigma^+$ ground state.

As is the case for other diatomic molecular ions, the near resonant product channel for electron capture of NO^+ from ground state Cs is the $3s\sigma$ Rydberg state. For the electronically-excited NO^+ states, these near-resonant product channels lie above the dissociation limit and give rise to the strong features observed in Fig. 1. However, for neutralization of the $NO^+ X^1\Sigma^+$ ground electronic state, the $(X^+)3s\sigma$ Rydberg state, $A^2\Sigma^+$, lies 1.02 eV below the dissociation limit and near-resonant DCT is possible only from rovibrational levels above v=3, N=26. The lowest energy product channels above the dissociation limit accessible to the ground vibrational level are the $(3p\sigma)X^+$ and $(3p\pi)X^+$ Rydberg states, which are labelled the $C^2\Pi$ and $D^2\Sigma^+$ states, respectively. Since production of these states requires an energy defect of order 1 eV for neutralization by ground state Cs, the charge transfer cross sections are small in comparison to the $3s\sigma$ channel. This large difference in cross section is the reason for the complete dominance in Fig. 1 of Rydberg series associated with NO^+ excited states, even though these states represent less than 50% of the ion beam.[10]

Observation of the fragments from the C and D states is problematic because the energy releases are so small. The D(v=0) state would produce fragment energy releases of only $W > 0.12$ eV and the releases from C(v=0) are yet smaller; C(v=0,N=3), the first level above the dissociation limit, would produce an energy release of only 0.0006 eV. Under the conditions in Fig. 2, the separations of such fragments lie below the cut-off of the detector and the peak that appears in the 12.5 V spectrum is actually the dissociation of C(v=1) with $W > 0.285$ eV. In order to effectively observe the low energy fragments, the apparatus was modified by extending the flight distance to the detector by an additional 100 cm, yielding a total flight distance L = 260.5 cm and a minimum detectable kinetic energy release of 60 meV from a 5 keV NO beam. Figure 2 shows the portion of the DCT spectrum in the range $0 \leq W \leq 0.5$ eV that was acquired with this extended flight distance at three pressures of NO in the ion source (3.5 mT, 7 mT, and 15 mT) and nominal 50 eV electron-impact ionization. For these spectra, the repeller field in the ion source was reduced to a minimum (~0 V). The combination of high NO pressure and long source residence time maximizes the number of ion-molecule reactions (charge-transfer) that can occur within the ion source and thus maximizes the amount of relaxation of the NO^+ beam. At the lowest pressure several distinct features appear in the spectrum that are labelled C(0), C(1), A(4), and D(1). The C(0) feature,

which lies at the lowest energy release, arises from neutralization of NO^+ X(v=0) to produce the C(v=0) $(3p\pi)X^+$ Rydberg state, which predissociates. Due to the detector cut-off, only rotational levels N > 14 are observable, but the combination of small W and long flight distance allows a complete resolution of the individual rotational levels, which appear as the sharp structure between threshold and W ~ 0.3 eV. At higher energy, the feature labelled C(1) arises from neutralization of NO^+ X(v=1) into the first excited vibrational level of the C state. The weak feature labelled D(1) may be evidence of capture into the corresponding level of the $(3p\sigma)X^+$ D state. Finally, the narrow feature labelled A(4) is associated with the near-resonant production of the $(3s\sigma)X^+$ A(v=4) Rydberg state from v=4 of the NO^+ ground state. This feature masks any possible contribution from D(0) in the low pressure spectra, since both levels would produce roughly the same energy release. Thus the DCT spectrum allows a full range of vibrational excitation in the NO^+ ion beam to be monitored. A comparison of the three spectra in Fig. 2 shows that features associated with the neutralization of vibrationally excited NO^+ rapidly decrease with increasing ion source pressure. Such a decrease over this range of pressure requires a rate constant for vibrational quenching of $\sim 10^{-10}$ cm^3/s. This rate is comparable to those measured[33] for vibrational quenching of O_2^+ in O_2, which would be expected from the similarities in the NO^+/NO and O_2^+/O_2 charge-transfer reactions.[34] In contrast, this rate is three orders of magnitude larger than that estimated from optical measurements.[14]

Somewhat higher resolution is achieved in the DCT spectrum by lowering the NO^+ ion beam energy to 4 keV. The resulting spectrum is shown in Fig. 3, which was acquired using 32 eV electron-impact on 15 mT of NO gas with minimum repeller field in the ion source. Two prominent features appear in the spectrum that can be uniquely assigned to the production and subsequent predissociation of the $(3p\pi)X^+$ $C^2\Pi$ Rydberg state in its ground and first excited vibrational levels. The intense low energy feature is highly structured, showing the resolution of the individual rotational levels in $C^2\Pi$(v=0). The apparatus resolution is roughly constant in $\Delta W/W$, hence the resolution has sufficiently degraded for the higher energy releases produced by the vibrationally excited $C^2\Pi$(v=1) levels that the individual rotational levels produce only an unresolved envelope. The stick spectra shown in the upper portion of the figure indicate the relative (apparent) populations and the absolute energy positions of the rotational levels in the two vibrational levels, that are obtained by fitting the observed kinetic energy release spectrum to the apparatus function and a rotational population distribution of 400K. The lowest energy feature in the $C^2\Pi$(v=0) feature corresponds to N = 13, but lies too close to the apparatus cutoff for its intensity to be considered reliable. The next higher rotational level, N = 14, is therefore chosen as the normalization point to obtain the relative intensities of the dissociation fragments from the two vibrational levels, yielding a ratio $C^2\Pi(v=1) : C^2\Pi(v=0) = 3.3\%$. The significance of this ratio

relies, however, on the dissociation rates of these Rydberg levels relative to their spontaneous emission rates. Tsukiyama et al.[35] have measured the lifetimes of the C(0) levels immediately above and below the dissociation limit and find decay rates consistent with the C(0) levels being >90 % predissociated. Furthermore, de Vivie and Peyerimhoff[36] have calculated that the predissociation rate for C(0) should increase with rotation. Therefore it is reasonable to expect that the population in the higher rotational levels observed here for C(0) accurately reflects the population produced in this state. The lifetime of the C(1) levels is found[37] to be more than an order of magnitude shorter than that of the predissociated levels in C(0); hence this vibrational level can be assumed completely dissociated. Thus, the relative intensities of C(0) and C(1) dissociation products should accurately reflect the relative populations in these levels and the relative vibrational populations in the ground electronic state of NO^+. In the absence of radiative cascade, direct ionization of NO is expected to produce a nascent population distribution in the NO^+ $X^1\Sigma^+$ v=0 and v=1 levels of 1 : 2, as observed in the photoelectron spectrum[38] and predicted from the Franck-Condon factors for the ionizing transitions. Thus the observed ratio of 1 : 0.033 demonstrates a rather complete quenching of vibrational excitation by collisions within the ion source.

One interesting aspect of the DCT spectrum in Fig. 3 is that only a very weak contribution is observed from the $D^2\Sigma^+$(v=0) level. Fragments from J=7.5 of this state contribute to a broadening of the fragment peak near W = 0.123 eV and fragments from J=14.5 are completely resolved as the small peak near W = 0.160 eV, as are several other rotational levels in the spectrum The $D^2\Sigma^+$ state is the (3pσ)X^+ Rydberg state and since its formation in the charge transfer neutralization of NO^+ X by Cs has nearly the same energy defect as that for the (3pπ)X^+ C state, one might expect it to appear at roughly 50% the intensity of the C state, reflecting its relative statistical weight, as is the case for formation of the (3pπ)X^+ $G^3\Pi_u$ and (3pσ)X^+ $D^3\Sigma_u^+$ states in N_2.[39] The very weak appearance of the $D^2\Sigma^+$ state here in the case of NO suggests that the ratio of its predissociation to radiation rate is quite small. This is consistent with the fluorescence measurements of Callear and Pilling.[40]

A second notable feature in the DCT spectrum is that the two spin-orbit components of the Rydberg C(0) state are strongly mixed with valence $B^2\Pi_{3/2}$(v=7) and must be described in terms of a p-complex[41] for rotational levels below N = 7. For the relatively high rotational levels observed here, the perturbation is insignificant and the C(0) can be treated as an independent state. This is underscored by the fact that no evidence of B(7) levels is observed in the DCT spectrum, as would be expected on the basis of its valence character in the higher rotational levels.

High vibrational excitation in the ground state of NO^+ is evidenced by the feature A(4) that appears prominently in the 3.5 mT spectrum shown in Fig. 2. At even lower pressures (not

shown) this feature is yet more prominent and the feature labelled D(1) both strengthens and narrows. Indeed, at low pressure the D(1) feature can be more appropriately be labelled A(5). As noted above, the $(3s\sigma)X^+$ Rydberg state $A^2\Sigma^+$ is the near-resonant product channel in the charge-transfer reaction of NO^+ $X^1\Sigma^+$ with Cs. Thus it allows a much more efficient transfer of ion population into neutral dissociation products. The appearance of A(4) in the DCT spectrum is the first evidence that this level dissociates. This contrasts with recent lifetime measurements[35] that concluded that the A state does not undergo predissociation. There is, however, some evidence to support predissociation. Tsukiyama et al.[35] have measured lifetimes for A(3) and A(4) of 164 ns and 137 ns, respectively, but have attributed the large decrease to the variation in the A-X transition moment with internuclear distance. Langhoff et al.[42] and more recently Sheehy et al.[43] have made *ab initio* calculations of the vibrational dependence in the A state radiative lifetime and predict less than a 2% difference in the radiative lifetimes of these two levels. If we attribute the much larger observed decrease to predissociation, then the A(4) level would be 16% predissociated. One unusual aspect of the A(4) feature is that it is quite narrow. Given that the rotational constant[44] for A(4) is comparable to that[45] of C(0), these features should exhibit a similar shape in the DCT spectrum. In reality, the A(4) feature is much narrower, with no evidence of high rotational levels. This suggests either that the predissociation rate for A(4) decreases with rotation or that the Rydberg character of this state decreases with rotation, thereby decreasing its charge-transfer cross section.

Finally, the utility of the cesium DCT spectrum in monitoring ion beam internal energy is illustrated in Fig. 4. The upper spectrum in this figure is the kinetic energy release produced by NO^+, created by 100 eV electron impact on NO gas at 0.1 mTorr, neutralized in Cs at a beam energy of 4 keV. In the lower portion of the figure is the kinetic energy release spectrum obtained under identical conditions, but with the NO^+ beam created by electron impact on n-Butyl nitrite (n-BuONO). Following measurements of the total charge transfer cross section of NO^+ with various targets at 2.8 keV, Thean and Johnson[46] have concluded that electron-impact on n-butyl nitrate produces a predominantly ground state NO^+ ion beam, whereas >40 eV electron-impact on NO gas produces 45% of the ion beam in long-lived NO^+ excited states. A comparison of the two spectra in Fig. 4 shows that indeed the population of electronically-excited NO^+ states is reduced by about a factor of three by preparing the beam from n-butyl nitrate. However, these excited electronic states are clearly not eliminated from the ion beam and the n-Butyl nitrite reagent also produces a degree of vibrational excitation in the ground state ions that is at least comparable to that formed by high energy electron impact ionization of NO gas.

ACKNOWLEDGEMENTS

This research was supported by Grant No. NAGW-360 from the NASA Space Sciences Branch. The work conducted at FOM is part of the research program of the "Stichting voor Fundamenteel Onderzoek der Materie" (FOM) and was made possible by financial support of the "Nederlandse Organisatie voor Wetenschappelijk Onderzoek" (NWO). This research was also supported by a travel grant from NATO.

REFERENCES

1. D. L. Albritton, A. L. Schmeltekopf, and R. N. Zare, J. Chem. Phys. **71**, 3271 (1979).
2. H. Partridge, S. R. Langhoff, and C. W. Bauschlicher, J. Chem. Phys. **93**, 7179 (1990).
3. O. Edqvist, E. Lindholm, L. E. Selin, H. Sjogren, and L. Asbrink, Arkiv Fysik **40**, 439 (1970).
4. O. Edqvist, L. Asbrink, and E. Lindholm, Z. Naturforsch. **26a**, 1407 (1971).
5. M. R. Manaa and D. R. Yarkony, J. Chem. Phys. **95**, 6562 (1991).
6. A. G. Calamai and K. Yoshino **101**, 9480 (1994).
7. R. F. Stebbings, A. C. H. Smith, and H. B. Gilbody, J. Chem. Phys. **38**, 2280 (1963).
8. T. F. Moran, F. C. Petty, and A. F. Hedrick, J. Chem. Phys. **51**, 2112 (1969).
9. T. O. Tiernan and R. E. Marcotte, J. Chem. Phys. **53**, 2107 (1970).
10. R. F. Mathis, B. R. Turner, and J. A. Rutherford, J. Chem. Phys. **59**, 2051 (1968).
11. I. Dotan, F. C. Fehsenfeld, and D. L. Albritton, J. Chem. Phys. **71**, 3289 (1979).
12. G. Ma, M. Suto, and L. C. Lee, J. Chem. Phys. **94**, 7893 (1991).
13. T. Kato, K. Tanaka, and I. Koyano, J. Chem. Phys. **79**, 5969 (1983).
14. F. Bien, J. Chem. Phys. **69**, 2631 (1978).
15. Y. K. Bae, M. J. Coggiola, and J. R. Peterson, Phys. Rev. A**31**, 3627 (1985).
16. W. J. van der Zande, W. Koot, J. Los, and J. R. Peterson, J. Chem. Phys. **89**, 6758 (1988).
17. K. P. Huber and G. Herzberg, *Molecular Spectra and Molecular Structure IV. Constants of Diatomic Molecules* (Van Nostrand Reinhold, New York, 1979).
18. D. P. deBruijn, J. Neuteboom, V. Sidis, and J. Los, Chem. Phys. **85**, 215 (1984).
19. D. P. deBruijn, J. Neuteboom, T. R. Govers, and J. Los, Phys. Rev. A **34**, 3847 (1986).
20. W. J. van der Zande, W. Koot, J. R. Peterson, and J. Los, Chem. Phys. Lett. **140**, 175 (1987).
21. W. J. van der Zande, W. Koot, J. Los, and J. R. Peterson, J. Chem. Phys. **89**, 6758 (1988).

22. W. J. van der Zande, W. Koot, and J. Los, J. Chem. Phys. **91**, 4597 (1989).

23. C. W. Walter, P. C. Cosby, and J. R. Peterson, J. Chem. Phys. **98**, 2860 (1993).

24. W. J. van der Zande, W. Koot, J. R. Peterson, and J. Los, Chem. Phys. **126**, 169 (1989).

25. W. van der Zande, W. Koot, D. P. DeBruijn, and C. Kubach, Phys. Rev. Lett. **55**, 1219 (1986).

26. H. Helm and P. C. Cosby, J. Chem. Phys. **86**, 6813 (1987).

27. D. P. deBruijn and J. Los, Rev. Sci. Instrum. **53**, 1020 (1982).

28. O. J. Orient and S. K. Srivastava, J. Phys. B **20**, 3923 (1987).

29. T. D. Märk, J. Chem. Phys. **63**, 3731 (1975).

30. D. Rapp and P. Englander-Golden, J. Chem. Phys. **43**, 1464 (1965).

31. One effect of this high repeller field is to accelerate a fraction of the electrons passing through the ion source to an energy higher than their nominal energy. This produces small populations in the NO+ beam in ion states whose ionization threshold is higher than the nominal electron beam energy. The effect of this can be seen in the figure as weak DCT features at low nominal electron impact energies.

32. R. J. Stubbs, T. A. York, and J. Comer, Chem. Phys. **106**, 161 (1986).

33. H. Böhringer, M. Durup-Ferguson, D. W. Fahey, F. C. Fehsenfeld, and E. E. Ferguson, J. Chem. Phys. **79**, 4201 (1983).

34. T. F. Moran, M. R. Flannery, and P. C. Cosby, J. Chem. Phys. **61**, 1261 (1974).

35. K. Tsukiyama, T. Munakata, M. Tsukakoshi, and T. Kasuya, Chem. Phys. **121**, 55 (1988).

36. R. de Vivie and S. D. Peyerimhoff, J. Chem. Phys. **92**, 3613 (1990).

37. O. Benoist D'Azy, R. Lopez-Delgado, and A. Tramer, Chem. Phys. **9**, 327 (1975).

38. D. W. Turner, C. Baker, A. D. Baker, and C. R. Brundle, *Molecular Photoelectron Spectroscopy, A Handbook of He 584 Å Spectra* (Wiley-Interscience, London, 1970) p.54.

39. A. B. van der Kamp, P. C. Cosby, and W. J. van der Zande, Chem. Phys. **184**, 319 (1994).

40. A. B. Callear and M. J. Pilling, Trans. Faraday Soc. **66**, 1618 (1970); Trans. Faraday Soc. **66**, 1886 (1970).

41. A. Lagerqvist and E. Miescher, Helv. Phys. Acta **31**, 221 (1958).

42. S. R. Langhoff, C. W. Bauschlicher, and H. Partridge, J. Chem. Phys. **89**, 4909 (1988).

43. J. A. Sheehy, C. W. Bauschlicher, S. R. Langhoff, and H. Partridge, Chem. Phys. Letters **225**, 221 (1994).

44. C. Amiot and J. Verges, Phys. Scripta **26**, 422 (1982).

45. J. E. Murray, K. Yoshino, J. R. Esmond, W. H. Parkinson, Y. Sun, A. Dalgarno, A. P. Thorne, and G. Cox, J. Chem. Phys. **101**, 62 (1994).

46. J. E. Thean and R. H. Johnson, Int. J. Mass Spectrom. Ion Phys. **11**, 197 (1973).

FIGURE CAPTIONS

1. Kinetic energy release spectra observed for a 4 keV NO^+ beam neutralized in Cs vapor with a fragment flight distance L = 164 cm. The NO^+ ions were produced by electron impact on NO gas, at low pressure (0.1 mT) and high repeller voltage (40 V/cm) to minimize quenching within the ion source, using eight electron acceleration voltages ranging from 12.5 V (bottom) to 100 V (top). Those features attributable to Rydberg states built on the ground state ion core appear only at W < 1 eV.

2. Kinetic energy release spectra observed for a 5 keV NO^+ beam neutralized in Cs vapor with a fragment flight distance L = 260 cm. The NO^+ ions were created by 50 eV electron impact on NO gas at three pressures and a minimum repeller field (~0.2 V/cm) in the ion source. Features identified with the n=3 Rydberg states of NO are labelled in the figure by the state name and vibrational quantum number.

3. Kinetic energy release spectrum observed for 4 keV NO+ neutralized in Cs with L = 260 cm. The ions were formed by 32 eV electron impact on NO gas at 15 mT pressure and minimum repeller field. Rotational level energies are given by the stick spectra in the upper portion of the figure for the $(3p\pi)X^+ C^2\Pi(v=0,1)$ and $(3p^s)X^+ D^2\Sigma^+(v=0)$ levels.

4. Kinetic energy release spectra observed for 4 keV NO+ neutralized in Cs with L = 164 cm. The NO+ beam for the upper spectrum was produced by 100 eV electron impact on NO gas at low (0.1 mT) pressure and high repeller voltage (40 V/cm). The NO+ beam for the lower spectrum was prepared under identical source conditions by electron impact on n-Butyl nitrite vapor.

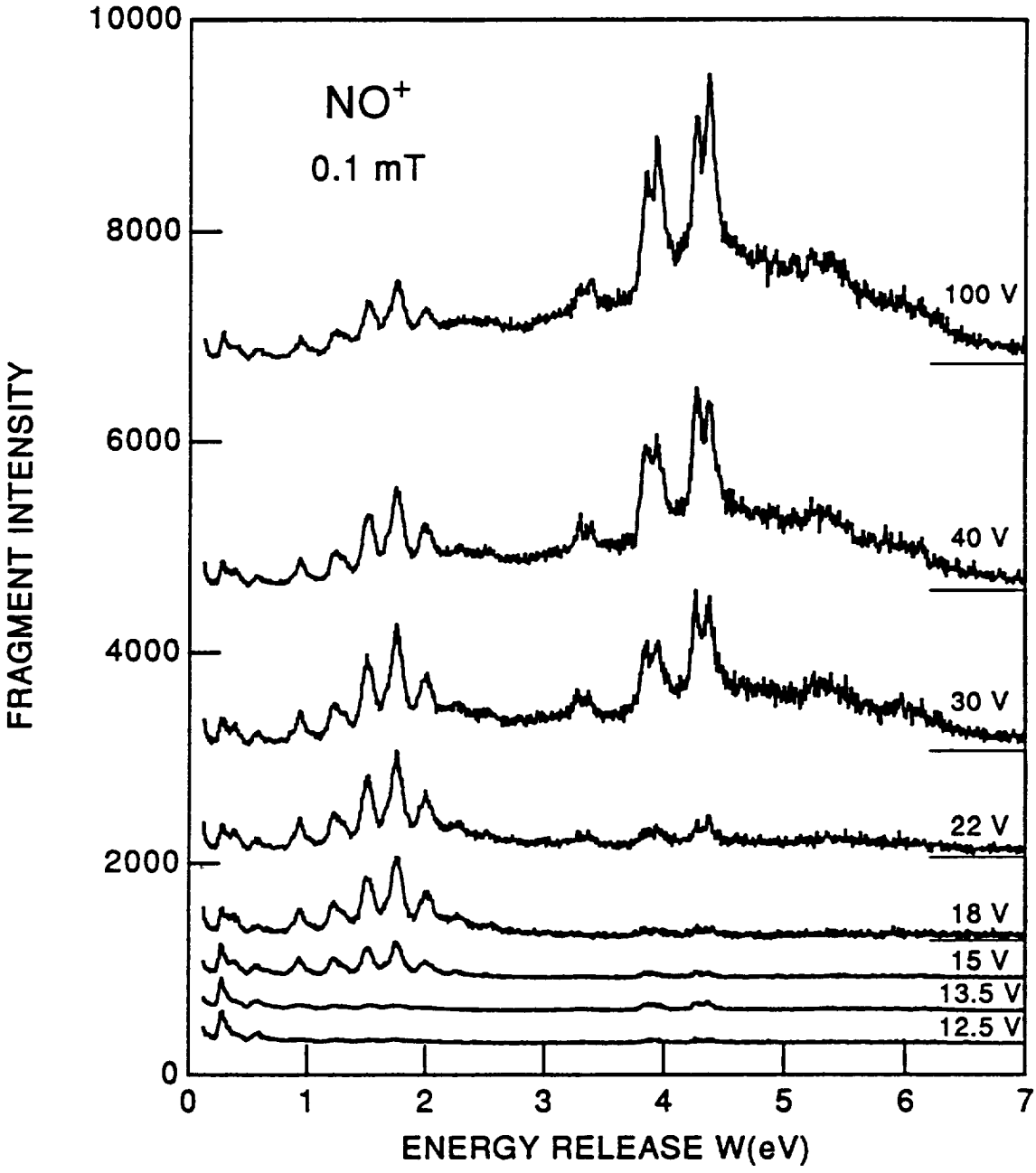
10000
8000
6000
4000
2000
0
NO+
0.1 mT
100 V
40 V
30 V
22 V
18 V
15 V
13.5 V
12.5 V
FRAGMENT INTENSITY
0
1
2
3
4
5
6
7
ENERGY RELEASE W(eV)

Figure 1

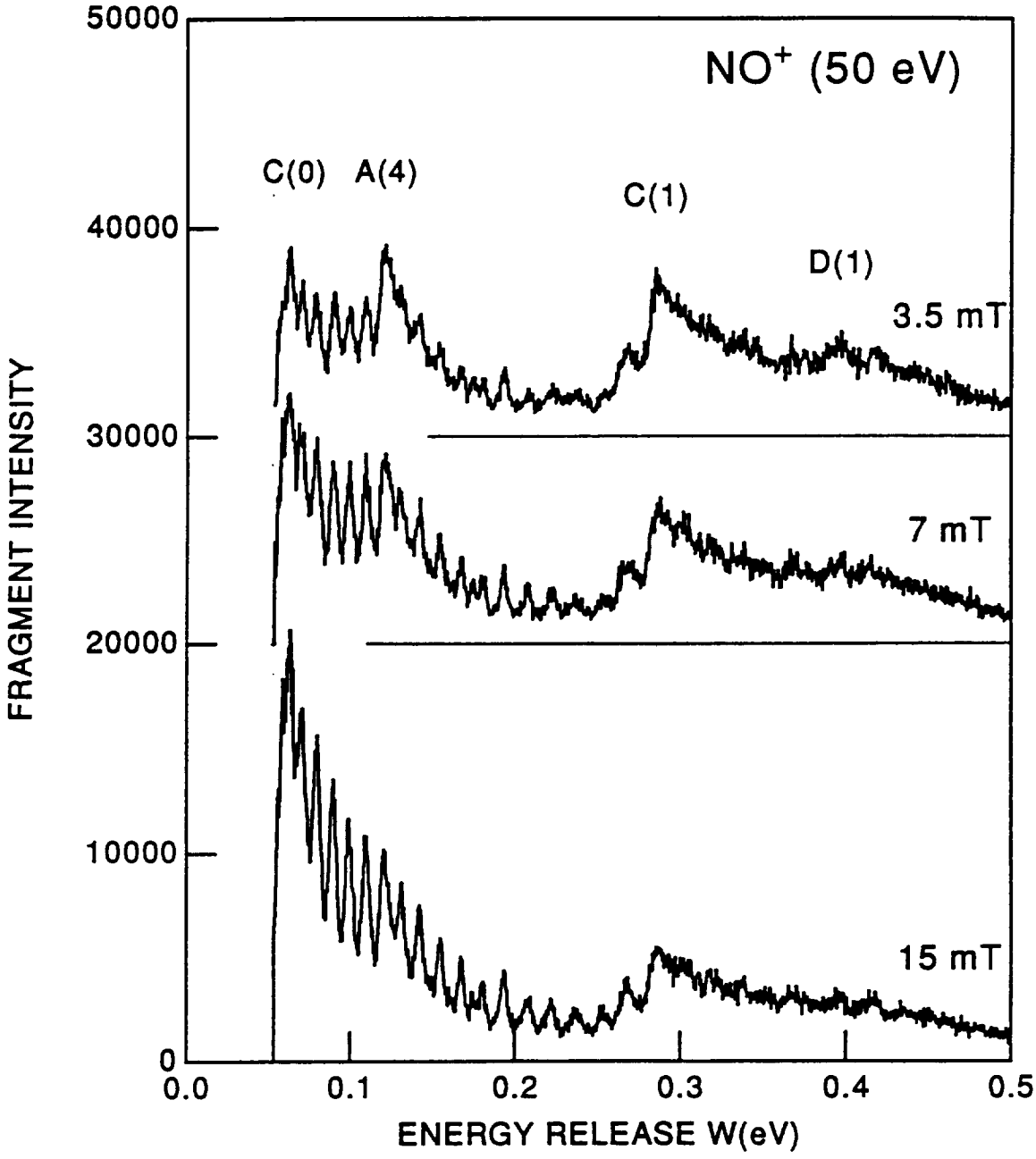
50000
40000
30000
20000
10000
0
FRAGMENT INTENSITY
NO+ (50 eV)
C(0)
A(4)
C(1)
D(1)
3.5 mT
7 mT
15 mT
0.0
0.1
0.2
0.3
0.4
0.5
ENERGY RELEASE W(eV)

Figure 2

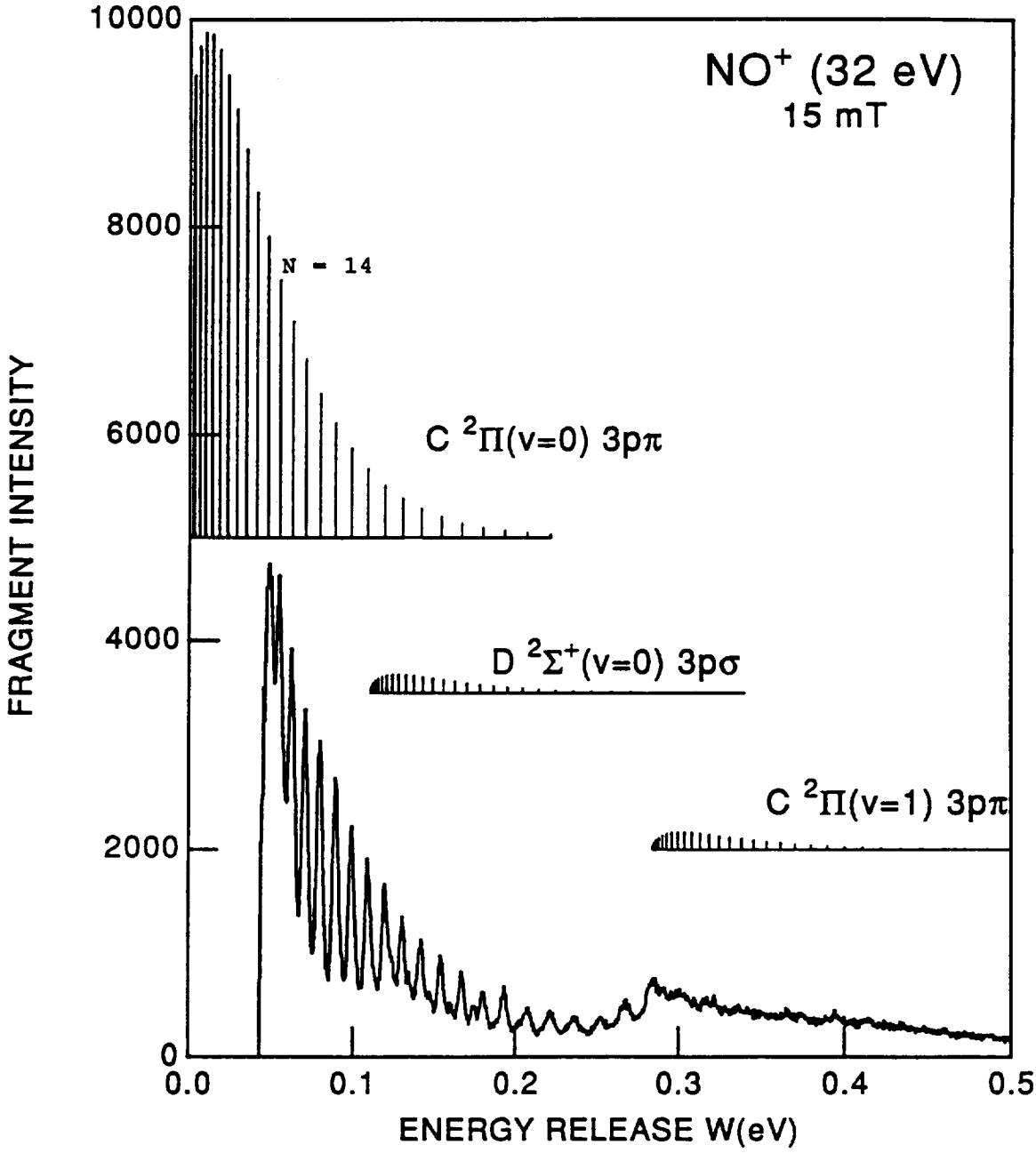
10000
8000
6000
4000
2000
0
FRAGMENT INTENSITY
NO+ (32 eV)
15 mT
N - 14
C 2Π(v=0) 3pπ
D 2Σ+(v=0) 3pσ
C 2Π(v=1) 3pπ
0.0
0.1
0.2
0.3
0.4
0.5
ENERGY RELEASE W(eV)

Figure 3

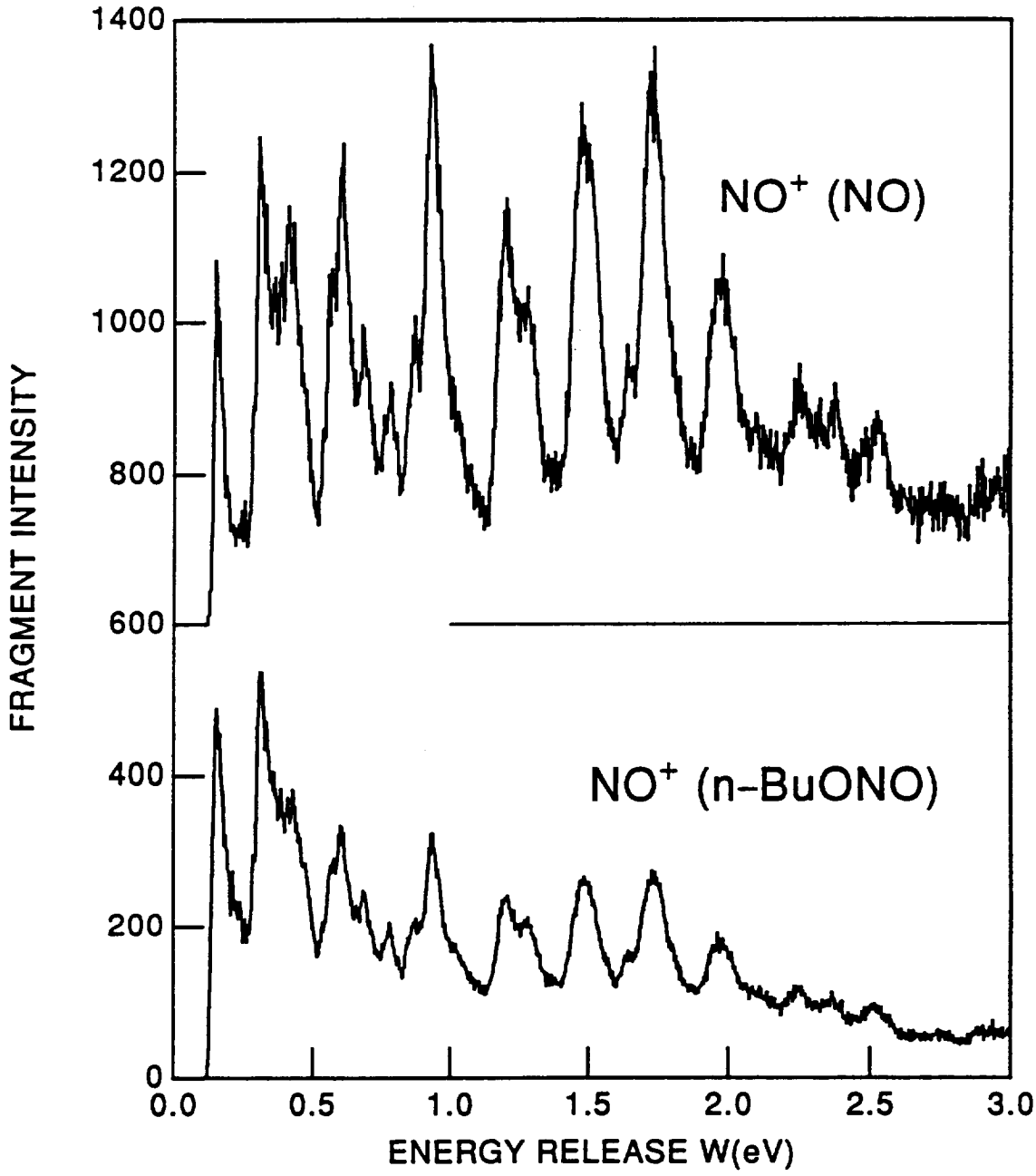
1400
1200
1000
800
600
400
200
0
FRAGMENT INTENSITY
NO+ (NO)
NO+ (n-BuONO)
0.0
0.5
1.0
1.5
2.0
2.5
3.0
ENERGY RELEASE W(eV)

Figure 4

APPENDIX C

DISSOCIATIVE CHARGE TRANSFER OF O_2^+ (v=0) IN Cs(6s) AND Cs(6p)

PRODUCTION OF A QUENCHED O_2^+ BEAM.

At very low ion source pressures and 100 eV electron impact, the O_2^+ ion beam arriving at the charge transfer cell is composed of two electronic states, $X^2\Pi_u$ and $a^4\Pi_u$, each with a rather broad vibrational population distribution.[1-3] For the case of charge transfer in Cs, the dominant process is near resonant electron capture into the 3sσ Rydberg states:

$$O_2^+(X^2\Pi_g,v^+) + Cs \rightarrow O_2\,(3s\sigma)X^+(v^*) \qquad (1a)$$

$$O_2^+(a^4\Pi_u,v^+) + Cs \rightarrow O_2(^{3,5}\Pi_u,v^*)\,(3s\sigma)a^+, \qquad (1b)$$

where X^+ and a^+ denote the electronic configuration of the molecular core of the O_2 Rydberg states: $X^+ = ...(3\sigma_g)^2(1\pi_u)^4(1\pi_g)^1$ and $a^+ = ...(3\sigma_g)^2(1\pi_u)^3(1\pi_g)^2$. The $(3s\sigma)X^+$ Rydberg states are the $C^3\Pi_g$ and $d^1\Pi_g$, which are separated in energy only by 0.1 eV and all levels of each are rapidly predissociated.[1] The $(3s\sigma)a^+$ Rydberg states are the $1^3\Pi_u$ and $1^5\Pi_u$ states, which are also near-degenerate. The $1^5\Pi_u$ state levels are rapidly predissociated. The $1^3\Pi_u$ state levels predissociate also, but autoionization effectively competes with this process in some of the vibrational levels.[2]

The ground vibrational levels in the $(3s\sigma)X^+$ states that dissociate to $O(^1D) + O(^3P)$ and $O(^3P) + O(^3P)$ give rise to fragments with kinetic energies of 1.07 eV and 3.03 eV respectively. On the other hand, the $(3s\sigma)a^+$ Rydberg states dissociating to these same limits give rise to fragments with kinetic energies of 5.33 eV and 7.01 eV, respectively. Higher vibrational levels in these states produce fragments with correspondingly higher kinetic energy releases. Since the product states are Rydberg states on the parent ion core, their rovibrational eigenstates are essentially identical to those of the ion. Consequently, the Franck-Condon factors for vertical transitions in the electron capture are diagonal ($v^* = v^+$) and the energy defect for the charge transfer reaction remains constant for each set of vibrational levels. As a result, the population distribution in the reactant ion beam is mirrored both in the population distribution of the Rydbergs and in the observed fragment intensities of the kinetic energy release spectrum. Although the branching among the accessible dissociation limits varies somewhat with state and vibrational level, a rather good qualitative indication of the population distribution in the $X^+(v=0\text{-}8)$ ions is obtained by the relative peak heights of the $O(^1D) + O(^3P)$ fragments that fall in the range of $1.1 \leq$

$W \leq 2.8$ eV. Similarly, the vibrational distribution in the a^+ ions is qualitatively given by the peak heights of the $O(^3P) + O(^3P)$ fragments that fall in the range $7.0 \leq W \leq 8.0$ eV. These individual vibrational levels are largely unresolved in the spectrum shown at the top of Fig. 1, which is obtained at very low ion source pressure with a minimum of quenching. It can be seen that the relative fragment intensities of the X^+ and a^+ Rydbergs are roughly comparable in this spectrum. Given that the concentrations of the X^+ and a^+ states are expected by be essentially equal in the unquenched O_2^+ beam,[3] the charge transfer cross sections must also be comparable.

As mentioned above, an extensive vibrational distribution is produced in both the X^+ and a^+ states by the process of 100 eV electron impact and the radiative cascade of short-lived excited states during extraction from the ion source and the 15 μs flight time to the charge transfer cell. In fact, contributions from high vibrational levels of the $(3s\sigma)X^+$ states dissociating to $O(^1D) + O(^3P)$ overlap those energy releases from the low vibrational levels dissociating to $O(^3P) + O(^3P)$ in the region of $W \sim 3$ eV. This vibrational excitation can be quenched by operating the ion source at higher O_2 pressures.

The resulting energy release spectra obtained at four different ion source pressures are shown in Fig. 1. It can be seen that increasing source pressure clearly affects the vibrational population distribution in the X^+ state, channeling more population into the ground vibrational level. This is expected from charge transfer reactions within the ion source:

$$O_2^+(X^2\Pi_g, v_r) + O_2(X^3\Sigma_g^-, v=0) \rightarrow O_2(X^3\Sigma_g^-, v) + O_2^+(X^2\Pi_g, v_p). \qquad (2)$$

The net effect of the reaction is to produce, on average, a product ion in a lower vibrational level than that of the reactant, $v_p < v_r$,[4] primarily because the vibrational spacing in the neutral is smaller than that in the ion. The rate constants for this quenching of $X^+(v_r=1)$ and $X^+(v_r=2)$ ions have been measured[5] to be 3×10^{-10} and 4×10^{-10} cm^3/s, respectively. At the highest pressure, 26 mT, nearly all of the X^+ population is in the ground vibrational level, with $\leq 10\%$ remaining in $X^+(v=1)$. In contrast, little if any, vibrational quenching seems to occur for the a^+ state levels, as evidenced by the shape of the feature near $W \sim 7.5$ eV, which remains largely unchanged at the various pressures, apart from decreasing in intensity. Several reactions of the a^+ ions are possible within the ion source:

$$O_2^+(a^4\Pi_u,v_r) + O_2(X^3\Sigma_g^-,v=0) \rightarrow O_2(X^3\Sigma_g^-,v) + O_2^+(a^4\Pi_u,v_p) \quad (3a)$$

$$O_2^+(a^4\Pi_u,v_r) + O_2(X^3\Sigma_g^-,v=0) \rightarrow O_2(A^3\Sigma_u^+,A'^3\Delta_u,v) + O_2^+(X^2\Pi_g,v_p) \quad (3b)$$

$$O_2^+(a^4\Pi_u,v_r\geq 4) + O_2(X^3\Sigma_g^-,v=0) \rightarrow O_3^+ + O \quad (3c)$$

The symmetric charge transfer reaction (3a) is probably rapid, however it has never been explicitly observed experimentally. It most likely does not lead to a vibrational quenching of the ions because the vibrational overlap between the lower vibrational levels of the O_2^+ $a^4\Pi_u$ and O_2 $X^3\Sigma_g^-$ states is poor and the vibrational spacing of the neutral is substantially greater than that of the ion. Thus (3a) would serve only to remove kinetic energy from O_2^+ $a^4\Pi_u$ during its drift through the ion source. In contrast, the near resonant channels in the asymmetric charge transfer reaction (3b) have very good vibrational overlaps and produce a conversion of the ion from the metastable $a^4\Pi_u$ state to the O_2^+ $X^2\Pi_g$ ground electronic state, most likely in its lowest vibrational levels. The rate constant for this reaction has been measured to be 3×10^{-10} cm^3/s at low collision energies,[6] which is comparable to the vibrational quenching rate of the ground state ion, Reaction (2), and roughly 1/3 of the Langevin (collision) rate. Finally, reaction of the metastable O_2^+ to produce O_3^+ is exothermic for levels above v_r=4. Dehmer and Chupka[7] have made a detailed study of the vibrational dependence of this reaction and estimate its rate at approximately ≤5% of the Langevin rate, i.e. at $\leq 0.5 \times 10^{-10}$ cm^3/s. Overall, the expectation of the O_2^+ $a^4\Pi_u$ reactions (3) are consistent with the observed loss of these ions with little quenching of their vibrational excitation, as indicated by the ker spectra in Fig. 1.

The changes in vibration population of the O_2^+ reactant that is probed by the Cs charge transfer reaction (1) can be modeled for the changes in ion source pressure by a solution of the coupled rate equations[8] for reactions (2) and (3) and the known rate constants for these reactions, given above, with the following presumptions: (a) the vibrational quenching of the O_2^+ X state occurs stepwise in single vibrational quanta, i.e. $v_p = v_r - 1$; (b) the quenching rates for $v_r > 2$ are 5×10^{-10} cm^3/s; (c) the vibrational distribution of X^+ produced by reaction (3b) is given by the $X^2\Pi_g(v) \leftarrow X^3\Sigma_g^-(v=0)$ Franck-Condon factors; and (d) the initial vibrational populations in O_2^+ $X^2\Pi_g$ and $a^4\Pi_u$ are those given in Table 1 of Walter et al [3] and Table 2 of van der Zande et al [2], respectively. From the known mobility of O_2^+ in O_2,[9] these rates are consistent with an effective applied electric field within the ion source of 0.2 V/cm, which presumably arises from contact potentials within the source volume and field penetration from the acceleration lens system.

From reaction (3b), the effect of O_2^+ $a^4\Pi_u$ state ions produced by the initial electron impact is to retard the vibrational quenching of the ground state ions. This is the primary reason why only ~90% of the ion beam is relaxed into the ground vibrational level at the highest practical source pressure of 26mT. A further reduction in the vibrational excitation requires the elimination of this precursor. This is accomplished by reducing the electron impact energy for the ionization from 100 eV to a value nominally below the threshold for the production of this state at 16.2 eV. The combination of high O_2 pressure and low electron impact energy was able to reduce the population in $X^+(v=1)$ to <3 % of the ion population, with immeasurably small populations in $v > 1$, as will be shown in a subsequent section. An equivalent degree of quenching can also be achieved by producing the X^+ beam in a high pressure hollow cathode discharge, as will be discussed below. At these low fractional populations, the ion vibrational populations derived from the DCT spectra can only be considered to be upper limits, due to the possibility of non-diagonal Franck-Condon transitions in the charge transfer reaction.

Note that the DCT spectrum of O_2^+ $X^2\Pi_g,(v=0)$ should consist of only two features: unresolved or partially resolved doublet features at W = 1.1 eV and W = 3.0 eV corresponding to the predissociation of the near-degenerate d,C $^{1,3}\Pi_g(v=0)$ levels to $O(^1D) + O(^3P)$ and $O(^3P) + O(^3P)$, respectively. These two features are in fact observed in the highest pressure spectrum of Fig. 1, but a number of other features also appear in the regions of W ~ 1.6, 2.3, and 4.3 eV. These features are identified as the predissociation of $(3p\lambda)X^+(v=0)$ Rydberg state levels.

LASER EXCITATION OF THE CS TARGET

Charge transfer reactions at keV energies are characterized by relatively large cross sections for the formation of product states that can be produced by the simple addition of a single electron to the reactant ion and for which the energy defect ε in the reaction is nearly zero. Such charge transfer reactions are described as near resonant, or resonant for the case of $\varepsilon = 0$. In this near resonant limit, the charge exchange takes place at large impact parameters, with little if any perturbation of the internuclear separation in the reactant ion. At keV energies, the time scale of the collision is short, compared to the nuclear vibrational period. Hence the product state vibrational distribution is characterized by the Franck-Condon factors for the recombination transition.

The advantages of Cs as a charge transfer target are twofold. First, the atom has a very large polarizability, which contributes a large attractive ion-induced dipole (R^{-4}) force to the charge-transfer collision. Secondly, the ionization potential of this species, which is the lowest of any stable, ground state atom, is 3.89 eV. The significance of this is illuminated if we consider the possible product states that would be produced by resonant charge transfer. For this case of zero energy defect, the product state must lie approximately[Kimura] 3.8939 eV below the reactant ion

state. Considering the traditional definition of Rydberg states, the resonance condition is met when the product state is a Rydberg state with an effective quantum number n* of:

$$n^* = n - \delta = \left(\frac{R}{IP_{target}}\right)^{\frac{1}{2}} , \qquad (4)$$

where δ is the quantum defect, R is the Rydberg constant (109735.4 cm^{-1} for O_2), and IP_{target} is the ionization potential for the charge transfer target. For the case of ground state Cs(6s) as the target, Eq. (4) yields an effective quantum number n* = 1.869, implying a quantum defect of δ = 1.131 for the lowest energy Rydberg state n = 3. This corresponds almost exactly to that expected for the 3sσ Rydberg states in most diatomic molecules, and is responsible for the facile production of the (3sσ)X^+ Rydberg states $d^1\Pi_g$ and $C^3\Pi_g$ and the (3sσ)a^+ Rydberg states for the present case of O_2. Changing the charge transfer target changes the IP, and therefore n*, for the resonant channel, but any increase in IP above that of Cs(6s) necessarily moves the region of resonance beyond the range of any Rydberg states. However, optical excitation of the Cs(6s) into an excited state, Cs*, effectively lowers the ionization potential, giving resonant access to Rydberg states with larger effective quantum numbers. In the present experiment, the Cs(6s) was optically excited to the 6p $^2P_{1/2}$ or $^2P_{3/2}$ states by pumping the resonance lines at 8946 Å or 8523 Å, respectively, with the beam of a Ti:Sapphire laser introduced into the Cs vapor oven colinear with the reactant ion beam. Reactions with these Cs* states give resonant access to n* = 2.329 or 2.362, i.e. to n=3 Rydberg states with quantum defects of δ = 0.671 or δ = 0.638, respectively. These are close to the expected 1^0 quantum defects of 0.54 and 0.68 for the 3pσ and 3pπ Rydberg states of O_2. In comparison to the reactions with ground state Cs, reaction with Cs* greatly increases the energy defect for the production of the 3sσ Rydberg states ($\delta \sim 1.1$) and greatly decreases that for the production of the 3dλ Rydberg states ($\delta \sim 0.1$). The expectation is that the magnitude of the charge transfer cross section varies inversely with the magnitude of the energy defect in the reaction.[11-13]

The effects of laser excitation of the Cs target at the 8523Å resonance lines is shown in Fig. 2. The spectrum was acquired by repetitively chopping the laser beam and separately accumulating the dissociation products during the laser on and laser off periods. The spectrum shown in Fig. 2 is the difference resulting from the subtraction of the fragments acquired during these two periods, with the d,$C^1\Pi_g$ feature near W = 1.1 eV and W = 3.0 eV in the laser-on spectrum normalized to the same features in the laser-off spectrum prior to subtraction. This normalization is necessary for clarity in the difference spectrum, because the smaller charge-transfer cross sections for producing the (3sσ)X^+ Rydberg states with Cs(6p) would otherwise

produce large, negative-going features for these states in the difference spectrum. As anticipated above, there is no effect on the DCT spectrum when the laser is tuned to a wavelength other than that within the absorption profile of the Cs resonance line (the difference spectrum is zero). When the laser is tuned to the resonance line, the magnitude of the spectral changes depends on the laser flux transmitted through the Cs vapor along the path of the ion beam. Due to the restrictions of the apparatus, the laser beam enters the vacuum system approximately 2 meters from the charge transfer cell and must the transmitted through the ion beam optics to reach the cell. Further, there was no way to monitor the fraction of laser power arriving at or passing through the cell, except for the changes it induced in the flux of dissociation fragments. Moreover, the (time-averaged) bandwidth of the laser (~0.3 cm^{-1}) was very much broader than the resonance line. As a result, fractional excitation of the Cs vapor varied with the (intrinsically unstable) distribution of transverse modes of the laser. Consequently, there was no way to quantitatively relate spectral changes to laser flux. Qualitatively, the spectral changes were roughly proportional to laser power and the distribution of the kinetic energy releases was independent of laser power and alignment.

Regarding the 3sσ features that appear as doublets in Fig. 1 at W ~ 1.1 eV and W ~ 3.0 eV, it is noted that they are depleted by the Cs* excitation and that the fractional change in each of these features is identical. This is expected since the intensity change in the energy release feature must reflect the change in population of the d,C (v=0) product state levels produced by the charge transfer. In contrast, the other features in the DCT spectrum are enhanced by the Cs* excitation, and it is noted that the degree of enhancement varies from feature to feature, and indeed, within features. The overall enhancement of these features demonstrates that they arise from the production of Rydberg states with higher effective quantum numbers than the 3sσ states. The preliminary identification of these states is shown in Fig. 2.

REFERENCES

1. W. J. van der Zande, W. Koot, J. R. Peterson, and J. Los, Chem. Phys. Letters **140**, 175 (1987).
2. W. J. van der Zande, W. Koot, J. R. Peterson, and J. Los, Chem. Phys. **126**, 169 (1989).
3. C. W. Walter, P. C. Cosby, and J. R. Peterson, J. Chem. Phys. **98**, 2860 (1993).
4. T. F. Moran, K. J. McCann, M. Cobb, R. F. Borkman, and M. R. Flannery, J. Chem. Phys. **74**, 2325 (1981).
5. H. Böhringer, M. Durup-Ferguson, D. W. Fahey, F. C. Fehsenfeld, and E. E. Ferguson, J. Chem. Phys. **79**, 4201 (1983).
6. W. Lindinger, D. L. Albritton, M. McFarland, F. C. Fehsenfeld, A. L. Schmeltekopf, and E. E. Ferguson, J. Chem. Phys. **62**, 4101 (1975).
7. P. M. Dehmer and W. A. Chupka, J. Chem. Phys. **62**, 2228 (1975).
8. T. G. Slanger and D. L. Huestis, Int. J. Chem. Kinet. **17**, 713 (1985).
9. R. M. Snuggs, D. J. Volz, J. H. Schummers, D. W. Martin, and E. W. McDaniel, Phys. Rev. A **3**, 477 (1971).
10. E. Lindholm, Arkiv Fysik **40**, 97 (1969).
11. D. Rapp and W. E. Francis, J. Chem. Phys. **37**, 2631 (1962).
12. A. B. van der Kamp, L. D. A. Siebbeles, W. J. van der Zande, and P. C. Cosby, J. Chem. Phys. **101**, 9271 (1994).
13. A. B. van der Kamp, J. H. M. Beijersbergen, P. C. Cosby, and W. J. van der Zande, J. Phys. B **27**, 5037 (1994).

FIGURE CAPTIONS

1. Kinetic energy release spectra observed from the charge transfer of 5 keV O_2^+ in Cs vapor for four pressures of O_2 gas in the electron impact ion source operating at 100 eV electron impact energy. Features appearing in the spectra with W < 5 eV and W > 5 eV arise from predissociated $3s\sigma_g$ Rydberg levels built on the O_2^+ $X^2\Pi_g(v)$ and $a^4\Pi_u(v)$ cores. Tick marks indicate the energy releases produced by specific vibrational levels in these states dissociating to $O(^1D) + O(^3P)$ and $O(^3P) + O(^3P)$ products. Additional features appear in the high pressure (26 mT) spectrum due to the nonresonant charge transfer production of $3p\lambda$ and $3d\lambda$ Rydberg states, as indicated in the figure.

2. Kinetic energy release spectrum observed from the charge transfer of 5 keV O_2^+ in laser-excited Cs(6p) vapor. The O_2^+ ion beam composition was >98% $X^2\Pi_g(v=0)$. The laser exciting the Cs vapor at 853 nm was chopped to acquire this spectrum. The cross sections for the production of O_2 Rydberg states at energies higher than $(3s\sigma_g)X^+$ are enhanced in the charge transfer with excited Cs. The energy releases and atomic product states produced by the predissociation of these Rydberg states are labeled.

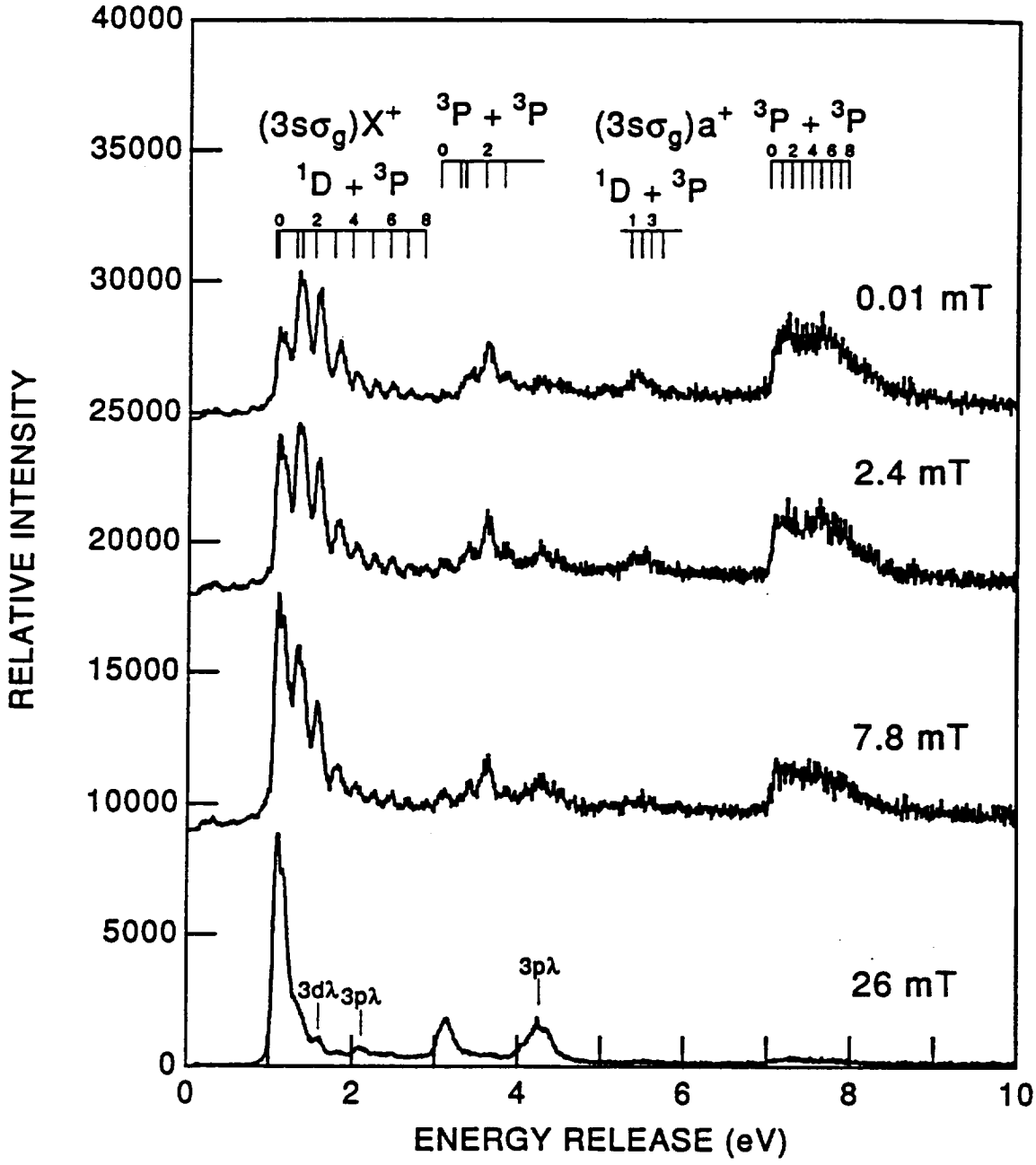
40000
35000
30000
25000
20000
15000
10000
5000
0
RELATIVE INTENSITY
$(3s\sigma_g)X^+$ $^3P + ^3P$
$^1D + ^3P$
0 2 4 6 8
0 2
$(3s\sigma_g)a^+$ $^3P + ^3P$
0 2 4 6 8
$^1D + ^3P$
1 3
0.01 mT
2.4 mT
7.8 mT
26 mT
3dλ
3pλ
3pλ
0
2
4
6
8
10
ENERGY RELEASE (eV)

Figure 1

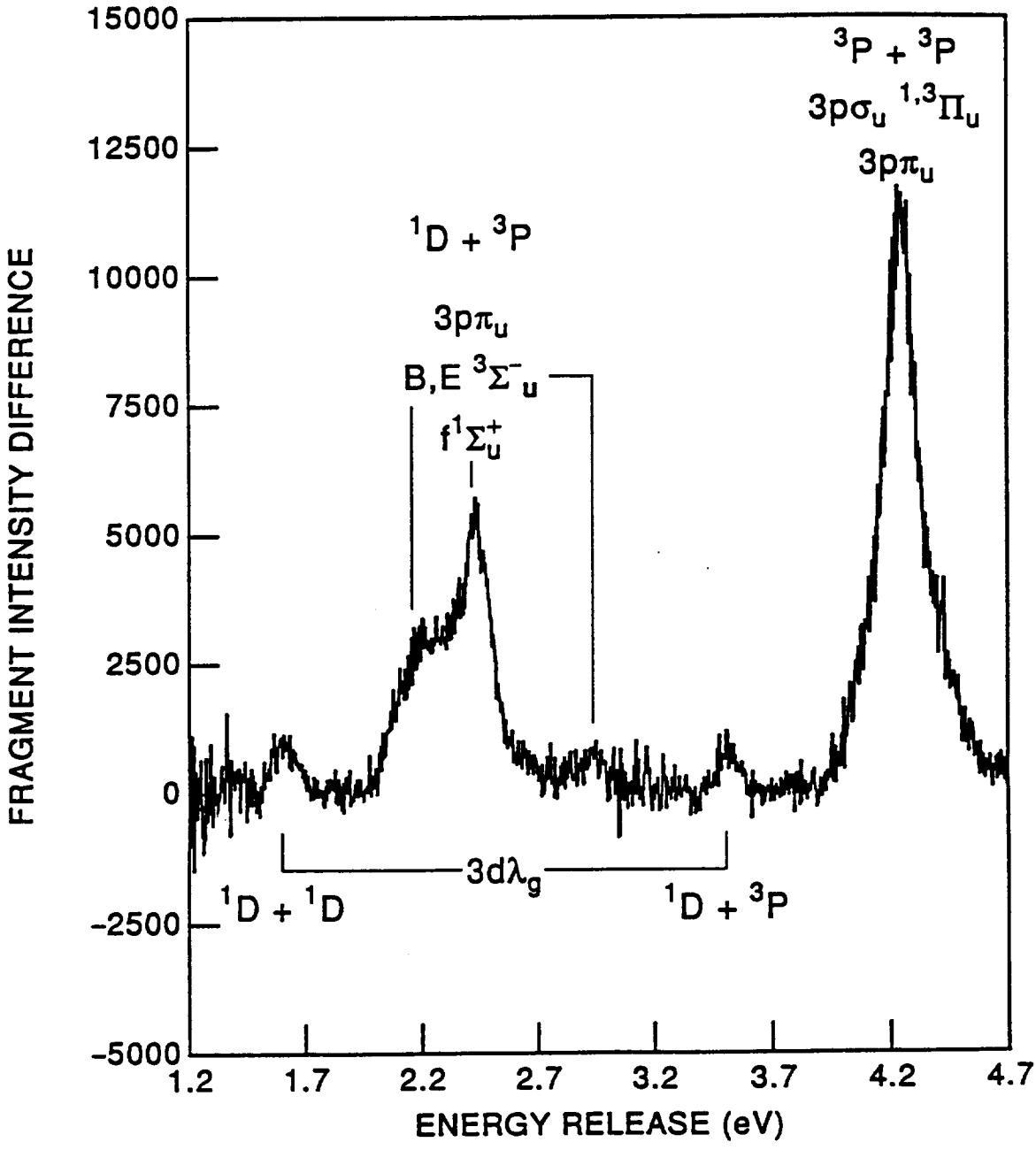
15000
12500
10000
7500
5000
2500
0
-2500
-5000
FRAGMENT INTENSITY DIFFERENCE
1.2
1.7
2.2
2.7
3.2
3.7
4.2
4.7
ENERGY RELEASE (eV)
$^3P + {}^3P$
$3p\sigma_u\ {}^{1,3}\Pi_u$
$3p\pi_u$
$^1D + {}^3P$
$3p\pi_u$
$B,E\ {}^3\Sigma^-_u$
$f\,{}^1\Sigma^+_u$
$3d\lambda_g$
$^1D + {}^1D$
$^1D + {}^3P$

Figure 2